University of Alberta

Evaluation of Brain Hypoxia with Radiolabeled Iodoazomycin Arabinoside (IAZA) in the Gerbil Stroke Model

By

Hui Liu ©

A thesis submitted to The Faculty of Graduate Studies and Research

in partial fulfillment of the requirements for the degree of

Master of Science

in

Pharmaceutical Sciences

Faculty of Pharmacy and Pharmaceutical Sciences

Edmonton, Alberta

Fall, 1997

National Library of Canada
Acquisitions and Bibliographic Services
395 Wellington Street
Ottawa ON K1A 0N4
Canada

Bibliothèque nationale du Canada
Acquisitions et services bibliographiques
395, rue Wellington
Ottawa ON K1A 0N4
Canada

Your file Votre référence

Our file Notre référence

The author has granted a non-exclusive licence allowing the National Library of Canada to reproduce, loan, distribute or sell copies of this thesis in microform, paper or electronic formats.

L'auteur a accordé une licence non exclusive permettant à la Bibliothèque nationale du Canada de reproduire, prêter, distribuer ou vendre des copies de cette thèse sous la forme de microfiche/film, de reproduction sur papier ou sur format électronique.

The author retains ownership of the copyright in this thesis. Neither the thesis nor substantial extracts from it may be printed or otherwise reproduced without the author's permission.

L'auteur conserve la propriété du droit d'auteur qui protège cette thèse. Ni la thèse ni des extraits substantiels de celle-ci ne doivent être imprimés ou autrement reproduits sans son autorisation.

0-612-22627-1

Canada

University of Alberta

Library Release Form

Name of Author: Hui Liu

Title of Thesis: Evaluation of Brain Hypoxia with Radiolabeled Iodoazomycin Arabinoside (IAZA) in the Gerbil Stroke Model

Degree: Master of Science

Year this Degree Granted: 1997

Permission is hereby granted to the University of Alberta Library to reproduce single copies of this thesis and to lend or sell such copies for private, scholarly, or scientific research purposes only.

The author reserves all the other publication and other rights in association with the copyright in the thesis, and except as hereinbefore provided, neither the thesis nor any substantial portion thereof may be printed or otherwise reproduced in any material form whatever without the author's prior written permission.

Hui Liu

3A-9002, 112St.
Edmonton, AB
Canada T6G 2C5

Date: Sept. 26th, 1997

THE UNIVERSITY OF ALBERTA

FACULTY OF GRADUATE STUDIES AND RESEARCH

The undersigned certify that they have read, and recommend to the Faculty of Graduate Studies and Research for acceptance, a thesis entitled: **Evaluation of Brain Hypoxia with Radiolabeled Iodoazomycin Arabinoside (IAZA) in the Gerbil Stroke Model**, hereby submitted by **Hui Liu** in partial fulfillment of the requirements for the degree of **Master of Science in Pharmaceutical Sciences**.

John R. Mercer.
Dr. John Mercer (Supervisor)

Allan Franko
Dr. Allan Franko

M.R. Suresh
Dr. M.R. Suresh

Dr. Steve McQuarrie (Exam Chair)

Date: Sept. 20th, 1997

DEDICATION

To my grandmother, Ms. Jiang Binyu, for her deepest love and affection for me.

To my father, Mr. Liu Hongyun, for his unparalleled determination, strict discipline and excellent teaching to lead his children into intellectual endeavor. He is the one, who teaches me to walk on the road of science. He is the architect in all my academic endeavors and it is him who always make my path easier through his unique examples along with love, guidance, and encouragement.

To my mother, Ms. Jiang Ailing, for her endless love, affection and faith made it all possible for me to acquire the knowledge through her hardships and sacrifices.

To my dearest younger sister, Bing, for her understanding and love for me. Her sincere effort to take care of our parents helped me to overcome my home-sickness and to concentrate on my studies.

ABSTRACT

Radioiodinated iodoazomycin arabinoside (IAZA) has been synthesized as a non-invasive marker for tumor hypoxia and has shown hypoxia-selective binding in variety of ischemic tissues. In the present study, a Mongolian gerbil stroke model is used to investigate the potential of IAZA in detecting brain ischemia.

In vivo biodistribution of ^{125}I-IAZA was performed in sham-operated (control) and surgically induced ischemic gerbils (ligation). The whole brain radioactivity in the ligation group was higher than that of the control group. This compound showed rapid whole-body elimination (> 92% in 24 hr) and blood clearance in both groups. An increased uptake was also noted in brain sections and brain anatomic sites in ligated gerbils in sectioning and microscopic autoradiography studies. This increased uptake in the forebrain regions, was positively correlated with the severity of brain damage as measured by a qualitative stroke index.

The above results are interpreted to indicate that ^{125}I-IAZA is selectively bound to ischemic/hypoxic brain tissue in ligated gerbils.

ACKNOWLEDGEMENTS

With pleasure and pride I have the honor to express my sincere gratitude to my supervisor Dr. John Mercer, Assistant Professor of the Faculty of Pharmacy, for his constant and thoughtful guidance, keen interest and conceptual development of this research project. His patient, encouragement, dynamic supervision as well as valuable discussion made it all possible in successful completion of this work. I am particularly thankful to him for his generous help in reading the thesis manuscript and in constructing figures given in this thesis. His enormous contribution in advancement of my academic career will always be remembered.

My thanks and appreciation are due to Dr. Allan Franko, Associate Professor of Oncology, Cross Cancer Institute, for his advice in various aspects of this work and also for his facilities to perform autoradiography studies. Thanks are extended to Mrs. Brenda Wolokoff for her patient and help in doing autoradiographic studies.

I am grateful to Dr. Mavanur R. Suresh and Dr. Steve McQuarrie, for their suggestions on the thesis.

My sincere thanks are extended to Herbert Lee, Kumar Piyush, Rezaul H. Mannan, Daria Stypinski and Hai Wei, for their help in

the initial labeling of the compound and *in vivo* biodistribution studies.

My thanks are also due to all the teachers and staffs of the Faculty of Pharmacy, for their good will and friendship.

I am specially thankful to Mr. Matthew Kong and Mr. & Mrs. C.Y. Wu, for their generous contribution in helping me to complete my study in Canada.

I wish to say "thank you very much" to all my friends, especially George, Teresa, Anita, Miao, Ying, Jim, Karima, Qiu, Ye, Luoke Shucai, Joan, Sineen, Byul, Mandy, and Sanjida for their support and encouragement.

The financial supports by the Faculty of Pharmacy in the form of teaching assistantship are gratefully acknowledged. This work was funded by a grant from University of Alberta Central Research Fund.

TABLE OF CONTENTS

Chapter Page

1. INTRODUCTION.....1

2. SURVEY OF RELATED LITERATURE.....4

2.1. NUCLEAR MEDICINE ASSESSMENT OF STROKE.....4

2.1.1. Stroke pathology 4
2.1.2 Evaluation and treatment of stroke patients.....5
2.1.3. The role of nuclear medicine in stroke.....8
2.1.3.1. CT and MRI 8
2.1.3.2. SPECT and PET 10
2.1.4. Imaging the ischemic penumbra 13

2.2. THE DEVELOPMENT OF HYPOXIA TRACERS.....16

2.2.1. The development of nitroimidazoles as hypoxia tracers.....16
2.2.2. Metabolic pathway of nitroimidazoles 19
2.2.3. Development and characteristics of iodoazomycin arabinoside 22
2.2.4. Hypoxia tracer studies in animal stroke models.....26

2.3. STROKE ANIMAL MODEL 27

2.3.1. Brain vasculature of the Mongolian gerbil.....27
2.3.2. Common carotid artery occlusion 31
2.3.3. Cerebral blood flow and metabolism following ischemia..... 32
2.3.4. Changes in blood-brain barrier following ischemia.....36
2.3.5. Factors affecting brain ischemia.....37

2.4. AUTORADIOGRAPHY.....39

2.4.1. The principle of autoradiography.....39
2.4.2. Components of autoradiography.....41
2.4.2.1. Specimen.....41
2.4.2.2. Emulsion.....41
2.4.2.3. Radioisotopes.....42
2.4.3. Autoradiography in the evaluation of stroke..... 43

3. EXPERIMENTAL.....45

3.1. MATERIALS..... 45

3.1.1. Chemicals, solvent and equipment.....45
3.1.2. Instruments.....45
3.1.3. Anesthetics and surgical tools..... 45
3.1.4. Materials used in autoradiography.....46
3.1.5. Radioisotope.....46
3.1.6. Animals.....46

3.2. METHODS.....47

3.2.1. Synthesis of IAZA.....47
3.2.2. Radiolabeling and purification of IAZA.....47
3.2.2.1. Pivalic acid melt exchange labeling.....47
3.2.2.2. Thin layer chromatography.....48
3.2.2.3. Purification of ^{125}I-IAZA.....48
3.2.3. Animal studies.....49
3.2.3.1. Surgical procedures for inducing ischemia.....49
3.2.3.2. Brain temperature and stroke index monitoring..50
3.2.3.3. Administration of radiopharmaceuticals.....52
3.2.3.4. Collection of tissue samples.....52
3.2.3.5. Counting and analysis of samples.....53
3.2.4. Autoradiography study.....54
3.2.4.1 Sample preparation..... 54
3.2.4.2. Tissue processing.....54
3.2.4.3. Dipping and development of slides..... 55

3.2.4.4. Hematoxalin & Eosin staining.....55
3.2.4.5. Data collection from autoradiographs.....56

3.3. STATISTIC ANALYSIS..... 56

4. RESULTS AND DISCUSSION..... 57

4.1. Chemistry.....57
4.2. Observation during surgery, artery occlusion and recovery.....61
4.3. Brain temperature changes.....63
4.4. Biodistribution and elimination.....65
4.5. Brain section study.....78
4.6. Microscopic autoradiography.....85

5. CONCLUSION.....95

6. BIBLIOGRAPHY.....98

7. APPENDICES.....113

LIST OF TABLES

Table 2.1. Octanol-water partition coefficients for MISO and its analogs.....23

Table 3.1. Form used to record brain temperature (°C) in control and ligation groups..... 50

Table 3.2. Form used to record neurological signs and stroke index..... 51

Table 3.4. Procedures for tissue dehydration..... 54

Table 4.1. DPM values and % of total activity of 10 TLC fractions of ^{125}I-IAZA sample # 96-08..... 59

Table 4.2. Results of IAZA labeling and purification..... 61

Table 4.3. Mean±S.D. brain temperature (°C) in the control and ligation groups.....64

Table 4.4. Biodistribution of ^{125}I-IAZA following i.v. administration in control groups with 2hr recovery at various time intervals.. 67

Table 4.5. Biodistribution of ^{125}I-IAZA following i.v. administration in ligation groups with 2hr recovery at various time intervals..68

Table 4.6. Thyroid radioactivity as percent injected dose of ^{125}I-IAZA/organ, in the ligation and control groups.....75

Table 4.7. Biodistribution of ^{125}I-IAZA in brain sections at 5hr following i.v. administration in control and ligation groups..... 81

Table 4.8. General data of animals used in autoradiography studies.....87

Table 4.9. Mean silver grains per grid (1mm^2) over autoradiographs in different anatomic sites in both control and ligated gerbils of the first group.....90

Table 4.10. Mean silver grains per grid (1mm^2) over a autoradiographs in different anatomic sites in both control and ligated gerbils of the second group.....90

Table 4.11. The ligation-to-control ratios of silver grains over different anatomic sites of the first group.....91

Table 4.12. The ligation-to-control ratios of silver grains over different anatomic sites of the second group.....91

LIST OF SCHEMES

Scheme 2.1. Sequence of the reduction and electron transfer process in nitroimidazoles..... 20

Scheme 4.1. Radiolabelling of iodoazomycin arabinoside..... 57

LIST OF FIGURES

Figure 2.1. General schematic presentation of blood vessels originating from the aorta and supplying the gerbil head and brain.....29

Figure 2.2. Detailed presentation of the two sources of blood vessels reaching the brain in the Mongolian gerbil.....30

Figure 2.3. Schematic diagram illustrating changes in CBF, tissue PO_2 and $CMRO_2$ during ischemia and in the recirculation period.....34

Figure 2.4. Generalized schematic diagram showing a vertical section through an autoradiograph.....40

Figure 4.1. TLC chromatogram of a ^{125}I-IAZA sample #96-08....58

Figure 4.2. Diagram showing radiochemical yield of ^{125}I-IAZA sample #96-08 by plotting % activity vs fractions.....58

Figure 4.3. Percent of total activity vs fractions of ^{125}I-IAZA sample #96-08.....60

Figure 4.4. Tissue to blood ratios of radioactivity in heart, lung and brain at various time intervals following i.v. administration of ^{125}I-IAZA in ligated gerbil.....72

Figure 4.5. Tissue to blood ratios of radioactivity in heart, lung and brain at various time intervals following i.v. administration of ^{125}I-IAZA in control gerbils.....72

Figure 4.6. Tissue to blood ratios of radioactivity in stomach, gut, liver, and kidney at various time intervals following i.v. administration of ^{125}I-IAZA in ligated gerbils.....73

Figure 4.7. Tissue to blood ratios of radioactivity in stomach, gut, liver, and kidney at various time intervals following i.v. administration of ^{125}I-IAZA in ligated gerbils.....73

Figure 4.8. Whole-body elimination of radioactivity following i.v. administration of ^{125}I-IAZA in control and ligation groups.....76

Figure 4.9. Blood clearance of radioactivity following i.v. administration of ^{125}I-IAZA in control and ligation groups.....76

Figure 4.10. Dorsal view indicating brain sections through frontal planes.....79

Figure 4.11. Percent of injected dose per gram of brain tissue at 5hr following i.v. administration of ^{125}I-IAZA in the ligation and control groups.....82

Figure 4.12. Brain-to-blood ratios of radioactivity at 5hr following i.v. administration of ^{125}I-IAZA in ligation and control groups.....82

Figure 4.13. Percent of injected dose per gram of brain tissue in brain sections (A-G) plotted vs. stroke index in the control and ligation groups.....84

Figure 4.14. Anatomic sites of six coronal brain sections used for counting silver grains.....88

Figure 4.15. Mean silver grains per grid (1 mm^2) over autoradiographs in different anatomic sites in both control and ligated gerbils of the first group.....92

Figure 4.16. Mean silver grains per grid (1 mm^2) over autoradiographs in different anatomic sites in both control and ligated gerbils of the second group.....92

LISTS OF ABBREVIATIONS

ACA	anterior carotid artery
ADC	apparent diffusion coefficient
ATP	adenosine triphosphate
AZR	azomycin riboside
AgBr	silver bromide
AgCl	silver chloride
AgI	silver iodine
BBB	blood-brain barrier
BCO	bilateral carotid artery occlusion
°C	degree Celsius
CA1	hippocampus sector 1
CBF	cerebral blood flow
CBV	cerebral blood volume
CCA	common carotid artery
$CHCl_3$	chloroform
$CMRO_2$	cerebral metabolic rate for oxygen
CNS	central nervous system
CT	computed tomography

CVD	cerebrovascular disease
DWI	diffusion-weighted imaging
DNA	deoxyribonucleic acid
dpm	decay per minute
eff.	efficiency
Emax	maximum energy
EtOH	ethyl alcohol
GBq	gigabecquerel
HMPAO	hexamethylpropylene amine oxime
hr	hour(s)
HPLC	high performance liquid chromatography
IAZA	iodoazomycin arabinoside
IAZR	iodoazomycin riboside
i.v.	intravenous
KBq	kilobecquerel
KeV	kiloelectron volt
LCGU	local cerebral glucose utilization
MBq	megabecquerel
MCA	middle cerebral artery

mCi	millicurie
MeOH	methanol
mg	milligram(s)
min	minute(s)
MISO	misonidazole
mL	millilitre(s)
mmol	millimole(s)
MRI	magnetic resonance imaging
NaI	sodium iodine
NaOH	sodium hydroxide
OEF	oxygen extraction fraction
PCA	posterior carotid artery
PCOA	posterior communicating artery
PET	positron emission tomography
pHi	intracellular pH
PI	perfusion imaging
SCeA	superior cerebellar artery
S.D.	standard deviation
SI	stroke index

SPECT	single photon emission computed tomography
$TcPO_2$	transcutaneous oxygen tension
TIA	transient ischemic attack
TLC	thin layer chromatography
uCi	microcurie(s)
UCO	unilateral carotid artery occlusion
UV	ultraviolet

1. INTRODUCTION

Stroke is one of the leading causes of death in North America. There are an estimated 600,000 stroke victims every year of which over 150,000 die.[1] The treatment of stroke and the rehabilitation of stroke patients is a big burden to health care budgets. The assessment of stroke severity and in particular the identification of ischemic versus infarcted tissue can allow timely intervention and aggressive treatments which will lessen permanent damage and speed recovery.

Following a stroke it is generally agreed that damaged tissue will consist of two zones: (1) a central ischemic zone that is destined to progress to infarction; (2) a bordering zone which is at risk to become infarcted.[2] The latter zone has recently been renamed the ischemic penumbra. If blood flow and oxygenation are not restored to ischemic tissue, it will progress to infarcted tissue. The logical therapy of acute ischemic stroke will focus on reoxygenating tissue at risk and minimizing the size of the infarction. Therefore, identification and localization of this viable ischemic tissues using nuclear medicine and radiopharmaceuticals appears to be helpful in the diagnosis and treatment of stroke patients.

With several new tracers (^{18}FDG, $C^{15}O_2$, $H_2{}^{15}O$, ^{11}CO, $^{15}O_2$) and positron emission tomography (PET), the ischemic penumbra can

be identified as an area with low cerebral blood flow (CBF) and a low cerebral metabolic rate for oxygen ($CMRO_2$) and an increased oxygen extraction fraction (OEF) at an early stage after stroke onset.[3] However, several limitations exist despite the excellent data provided by PET. Two magnetic resonance image (MRI) techniques, diffusion-weighted imaging (DWI) and perfusion imaging (PI) also have shown promise for identification of ischemic penumbra, but these techniques are still under investigation.[4]

Another approach for detecting the ischemic penumbra is radioactive tracers that selectively bind to hypoxic areas. Over the past two decades, there has been a variety of research towards the goal of identification of ischemic/hypoxic tissue by using radiopharmaceuticals. Nitroimidazoles first appeared in clinical radiology as radiosensitizers and a number of radiolabeled analogs were then found to have favorable properties in terms of selective binding to hypoxic tissues.[5] One such analog is misonidazole(MISO) labeled with ^{18}F(1) which has been studied in both animals and preliminary clinical trials.[6,7] ^{18}F-MISO was observed to be retained selectively in viable ischemic tissue. However, its utility is limited by the short half-life of ^{18}F (110 min) and by the specialized PET imaging instrumentation requirement.

A radiolabeled sugar-coupled 2-nitroimidazole (2) (iodoazomycin arabinoside: IAZA) was synthesized as a non-invasive, scintigraphic

marker of tumor hypoxia few years ago.[8] Its unique physical-chemical and biological properties along with its hypoxia-selective binding characteristics make this compound promising for non-invasive diagnosis of tumor hypoxia. It has undergone extensive investigation in hypoxic cell culture, in animals, and in clinical trials of cancer patients.[9-11] The results of these studies are very encouraging, and suggest the usefulness of IAZA for detecting hypoxia not only in tumor tissue but also in other tissues such as ischemic myocardium and brain.

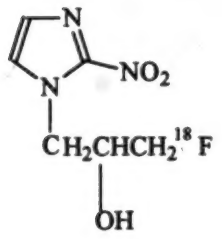

1

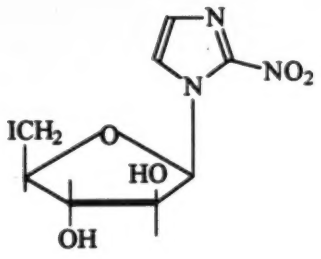

2

The previous studies of IAZA have led us to the investigation of this compound in the present stroke study. By careful analysis of the uptake of the compound into the brain tissue of the stroke animal, it should be possible to identify the region of hypoxia. The subject of this thesis is to reveal the potential of radiolabeled IAZA to detect hypoxic tissue in the brain.

2. SURVEY OF RELATED LITERATURE

2.1. NUCLEAR MEDICINE ASSESSMENT OF STROKE

2.1.1. Stroke Pathology

Stroke is the most common life-threatening neurologic disease and is one of the leading causes of death in North America.[1] Over the past 40 years, our knowledge on the pathophysiology and mechanisms of stroke has expanded rapidly; and progress has been made in the pharmacological and surgical treatment for stroke. However, there is at present no adequate therapy for stroke. Further investigations by research scientists and clinicians will be required to provide new tools and procedures to diagnose and treat this serious disease.

In stroke patients, there are two major types of brain damage: ischemia and hemorrhage. Ischemic stroke involves three different mechanisms: thrombosis, embolism, and decreased systemic perfusion. This type of stroke occurs most frequently, being responsible for more than 65% of the total incidence.[1]

Many physicians view ischemic stroke as a "cerebrovascular accident" caused by the homogeneous loss of blood supply, oxygen tension, and high energy metabolites in an area of brain that will inevitably become infarcted. Fortunately, many neurologists have observed patients with acute hemiparesis who recovered normal

motor function. This notion of reversible brain injury has stimulated clinical research to unravel the pathophysiology of focal brain ischemia and to develop new treatments to protect the brain against evolving ischemic necrosis.

It is in this setting that the "ischemic penumbra", that zone of ischemically threatened tissue adjacent to the core zone of an evolving ischemic infarction, was introduced into stroke research.[2] A more physiologically accurate definition of the ischemic penumbra is: the brain area with CBF decreasing to the point of causing electrophysiological silence but with preserved membrane potentials, ionic homeostasis and energy metabolism.[12] This border zone of ischemic tissue may exist up to 48 hours after stroke.[13] The ischemic penumbra is very important because it implies that focal ischemic injury is a dynamic process and that timely intervention by reperfusion or by drug therapy might be possible. However, in patients with acute stroke, clinical examination can not distinguish between the areas of severe ischemia with energy failure and developing infarction, and areas of less severe ischemia in penumbra with electrical failure and with the possible potential of recovery.[2] Ischemic/hypoxic tissue imaging tracers are well suited to this task because they will specifically identify tissue that is viable in an environment of diminished blood and oxygen.

2.1.2. Diagnosis and Treatment of Ischemic Stroke Patients

Previously, the diagnosis and evaluation of stroke was based chiefly on clinical syndrome, neurological examination, and coexisting risk factors of the patients. The diagnostic accuracy of the classification of ischemic stroke has rapidly evolved with the advancement of technologies to image the brain and blood vessels. With the widespread application of computed tomography (CT), magnetic resonance imaging (MRI), single photon emission computed tomography (SPECT), positron emission tomography (PET) and other diagnostic studies, the clinical impressions have been refined and supported by laboratory confirmation of the stroke subtype.[14]

In most hospitals the first step taken when a patient presents suspected stroke is to try to image the injured site by CT or MRI. These initial scans should differentiate hemorrhage from ischemia or infarction.[14] Duplex and transcranial doppler may disclose high grade stenosis of a carotid or vertebral artery before brain imaging demonstrates the changes due to infarction in the early hours after stroke.[15] On the other hand, angiography remains the preferred tool for differentiating embolism from large artery thrombosis, and for demonstrating aneurysms and vasospasm.[14] Applied quickly after stroke, ^{99m}Tc-HMPAO and ^{123}I-IMP SPECT studies demonstrate the deficit in local cerebral blood flow before the tissue signal changes appear on CT or MRI scan. ^{18}FDG and $^{15}O_2$ PET studies have also shown their power in documenting the functional metabolic response

of the brain to focal infarction, but their availability remains limited to PET centers.[16]

The development of these new techniques has also had a major impact on treatment decisions for all types of stroke. The mortality and morbidity from stroke has declined in a dramatic way: nearly 50% in 25 years.[17] A series of drugs that affect the process of thrombosis have been used in stroke patients and have been evaluated in the prevention of stroke. Encouraging evidence has been accumulating that establishes treatment strategies with the use of anticoagulants and platelet-inhibition agents. Anticoagulants have been reappraised for their benefit in atherothrombotic stroke and their use in progressing stroke.[18] Antiplatelet therapy is commenced immediately in most patients with acute strokes who are not candidates for anticoagulation.[18] Other drugs, such as vasodilators, continue to be used widely in the acute treatment of strokes. Glutamate and calcium antagonists have also given encouraging results in experimental ischemia.[19] The search for better therapeutic agents and strategies continues.

The ischemic penumbra has drawn a lot attention lately because of its possible potential for rescue. The interest in this region and its response to therapy arises from our understanding that following interruption of blood flow to the brain, a penumbra zone exists between the most densely ischemic core and the more normally perfused brain. This region is presumed, therefore, to contribute to

the clinical deficit, yet to be capable of responding to therapeutic intervention. Nonetheless, drug treatments that lead to reperfusion and that are targeted against biochemical changes contributing to ischemic damage, so far have not shown overwhelming success.[13,20] The problem is, however, being approached by the development of better imaging and new intervention techniques.

2.1.3. The Role of Nuclear Medicine in Stroke

Cerebrovascular disease (CVD), especially ischemic stroke, has always formed one of the main topics in nuclear medicine. Conventional brain scanning was used to detect the location and extent of lesions, but became obsolete with the advance of three-dimension imaging modalities, such as CT and MRI. Functional imaging and quantification of physiologic variables, are very useful in CVD since these changes are concomitant with vascular disorders and can be measured and followed in the course of stroke.

2.1.3.1. CT and MRI

Ambrose published the first clinical paper devoted to computed tomography (CT) in 1973.[21] In the following years, numerous papers dealing with different aspects of stroke clarified most of the CT features that are encountered in patients with transient ischemic

attack (TIA), ischemic or hemorrhagic infarction, and intracranial hemorrhage. CT is safe, non-invasive, and in some instances, can complete the neuroradiologic workup. On CT scan infarction, appearing as a low-density focus, occurs as early as 3 hours[22] but more often does not make an appearance before 6 hours. Within 3 days, it reaches a plateau in more than 60 percent of cases.[23] CT performed with or without contrast, is usually the first examination in stroke patients, whether ischemic or hemorrhagic, and is very valuable in orienting the subsequent diagnostic and therapeutic approach. However, CT not only shows low sensitivity in identifying the ischemic lesion during the critical first few hours after onset, but also does not reliably separate a deep lesion due to thrombosis from one occluded by embolism.[14]

MRI is based on the interaction between radio waves and certain nuclei of the body tissue, in the presence of a powerful magnetic field. [23] MRI has become, for many, the preferred technique of brain imaging because of the wealth of information it offers. Also, recent techniques have remarkably shortened imaging time and have become capable of selectively depicting the vascular anatomy and tissue perfusion, thereby opening the possibility of evaluating the reversibility of an infarction.[24] MR scanning offers a clear advantage over CT for imaging flowing blood, which appears black on the MR, allowing a diagnosis with a high degree of accuracy.[25] An early study by Kertesz et al[26] with 87 patients showed that MRI was more

sensitive than CT for the detection of infarction (90% vs 58%). MRI also has advantages over CT for the identification of smaller infarcts deep in the brain and those in the brain stem.[27] Nonetheless, MRI suffers the same problem as CT in that both methods are less adaptable to measuring perfusion changes and biochemical processes.[23] In addition, the expense and availability of this technology are limiting factors for its routine clinical application.

2.1.3.2. SPECT and PET

CT and MRI are valuable diagnostic techniques for defining structural changes in the brain. Since changes in perfusion usually precede structural changes, PET and SPECT imaging of brain function offers the potential for earlier diagnosis and subsequent intervention. Individually emitted and thus spatially and temporally uncorrelated radiation, such as gamma-rays associated with isomeric transition or electron capture as well as X-rays associated with electron capture or internal conversion, form the basis of SPECT.[28] SPECT has some advantages, when compared with PET, that make it widely used in research and clinical practice. Included in these are the longer half-life for the major medically useful radionuclides and the more readily available and less expensive instrumentation.

The measurement of CBF in patients with CVD was the earliest application of SPECT of brain. In the last decade, a variety of

studies have reported that SPECT shows the brain lesion earlier than does CT, and it may help to predict the outcome of stroke as well as to differentiate stroke pathogenesis.[28-30] By 8 hours after infarction, only 20% of CT scans will be positive, while about 90% of SPECT CBF scans will be abnormal at the same time interval.[28,29] The difference in sensitivity between structural and functional imaging modalities disappears within about 72 hours. [30]

Of the flow tracers designed for SPECT imaging, ^{99m}Tc labeled HMPAO (hexamethylpropylene amine oxime) is currently the most frequently used agent.[31] It has been postulated that HMPAO distributes in proportion to regional CBF.[31] Therefore, increased uptake of HMPAO may reflect a "luxury perfusion" which appears during a period lasting from several days to 3 weeks after stroke.[32,33] This situation is thought to reflect the breakdown of regulatory mechanisms and no benefit can be expected from increasing CBF.[33] Although the HMPAO SPECT scan can demonstrate the well-defined region of decreased perfusion in acute stroke patients, it can not distinguish the ischemic penumbra from an irreversibly damaged region, since CBF decreases in both regions at early stage of stroke.[34] However, it has been reported that ^{123}I-labeled glucose analogs bind to hypoxic tissue and may permit brain SPECT to identify the viable tissue.[34]

Up to now, no metabolic variable but CBF has been measured

routinely with SPECT. It is obvious therefore that single SPECT studies render only limited information in acute stroke. However, the introduction of PET as a powerful imaging modality has played a major role in the understanding of pathophysiologic mechanisms contributing to ischemic stroke.

PET scanning is based on the use of radiotracers that decay by the process of positron emission.[35] Modern scanners with high spatial resolution and dynamic capabilities, and a large variety of tracers are now available for the quantitative in vivo measurement of cerebral blood flow (CBF), cerebral metabolic rate for oxygen ($CMRO_2$), oxygen extraction fraction (OEF), cerebral blood volume (CBV) and intracellular pH (pHi).[35] Using these techniques, it is possible to characterize the balance between cerebral hemodynamics and cerebral metabolism in different stages of stroke. In addition, PET has allowed the development of new functional concepts on the therapy of acute brain ischemia and on mechanisms of functional recovery.[35]

Several studies applying $^{15}O_2$ and $C^{15}O_2$ for PET were performed during early infarction (first hour to 3 days).[35-38] In the core of infarction there is evidence that CBF and $CMRO_2$ below a certain threshold, 12 mL/100g /min and 65 umol/100g/min respectively, indicated irreversible tissue damage. In the border zone of ischemia (ischemic penumbra), the preservation of $CMRO_2$ with decreased CBF

resulting in increased OEF suggests that tissues are still viable up to 48 hours after stroke onset.[35-38] With few exceptions, these viable tissues suffer progressive metabolic derangement and turn necrotic in most instances during the following two weeks.[35-38] Although the therapeutic routines usually applied today can not prevent subsequent metabolic derangement and progression to necrosis, these viable tissues remain a target for timely treatment leading to the reduction of damage in ischemic stroke.[20, 39] Studies identifying viable tissue could be of value in the development of effective therapeutic strategies.

Despite the attractive features associated with PET, the short half-life of radiotracers as well as the expense and on-site cyclotron requirement, limit the clinical application of this technique to only in some major university medical centers and national laboratories in Canada.

2.1.4. Imaging the Ischemic Penumbra

There is great evidence that an ischemic penumbra exists in animals and humans after the occurrence of focal brain ischemia.[12,40] The concept of the penumbra leads to the idea of a therapeutic time window. If the region of irreversible injury (infarction) after focal ischemia evolves in time and space, then the possibility of interventional therapy becomes a tenable hypothesis. All of the acute stroke therapies given after stroke onset have their basis from this hypothesis of a therapeutic time window.[40]

Evidence for the existence of the ischemic penumbra is available from PET studies of both animal stroke models and stroke patients.[3,41] With PET, infarcted tissue can be identified as a region of low CBF, low $CMRO_2$ and low OEF. This combination of changes clearly indicates widespread infarct at 24 hours and has been confirmed by postmortem examination.[3,41] In the ischemic penumbra, however, there was a marked regional decline in CBF and $CMRO_2$ and an increase in OEF at early hours after stroke onset.[3,41] These PET studies in animal models also suggest that reversible condition in the penumbra may persist for many hours after the artery occlusion and that, in some patients, the time window for therapeutic intervention may be considerably longer than the currently hypothesized 4 to 8 hours.[3,41] Several limitations persist despite the excellent data provided in these studies. It remains unclear what precisely is the time course of the penumbra, as defined by PET parameters.[41] Additionally, the availability of PET is limited and ready access to PET facilities is problematic for acute stroke patients, as is the performance of multiple repetitive studies.

Two new MRI techniques, diffusion-weighted imaging (DWI) and perfusion imaging (PI), appear to be promising for the rapid identification of the ischemic penumbra and associated perfusion deficit.[4] In animal stroke models, the apparent diffusion coefficient (ADC) of tissue water that forms the basis for the signal intensity changes on DWI was observed to decline rapidly early after stroke

onset and was related to CBF reduction and high-energy metabolism failure.[42,43] In humans, the situation is likely to be much more complex than in those animal models, but a heterogeneity of ADC value should be seen early after stroke onset.[43] This information could possibly be used to image the penumbra versus infarcted tissue, if we can determine what ADC values can make this distinction in time and space.[42,43] In the future, the combination of diffusion and perfusion imaging data from MRI should provide valuable information to grade the severity of compromised blood flow and its consequent tissue effects.

Another approach for the identification of ischemic but salvageable tissue are tracers that selectively bind to hypoxic areas. MISO derivatives may be such substances and these analogs can be labeled with a variety of radionuclides to allow nuclear medicine imaging.[44] ^{18}F-MISO and ^{99m}Tc-complex of 2-nitroimidazole were observed to be retained selectively within the potentially reversible ischemic tissue after carotid artery occlusion.[6,44] A preliminary clinical trial in acute stroke patients also reported the feasibility of using ^{18}F-MISO to detect ischemic penumbra in vivo.[7] However, its practical use is limited by the short half-life of ^{18}F (110 min) and by the instrumentation requirement. A series of ^{125}I/^{123}I labeled sugar-containing MISO analogs have shown promise in identifying the viable ischemic tissue. These tracers have been demonstrated to have selective uptake into hypoxic tumor tissue in both animals and

cancer patients.[8-11] The results indicate the potential of employing these agents in detecting ischemic penumbra in acute stroke patients.

At present, the uncertainty about the time course of ischemic tissue damage and the location of potentially salvageable ischemic tissue remains. We still require a convenient and reliable mechanism to determine if a patient has viable ischemic tissue as guide for interventional therapy. The availability of an imaging modality that could indicate the presence and extent of these tissues would greatly facilitate stroke therapy trials and the selection of patients when proven therapies are available. The new MRI techniques and hypoxia tracers might afford this possibility. It is incumbent upon basic stroke researchers and clinicians to continue to define the ischemic penumbra and to develop readily applicable mechanism to identify and treat it.

2.2. THE DEVELOPMENT OF HYPOXIA TRACERS

2.2.1. The Development of Nitroimidazoles as Hypoxia Tracers

A considerable effort has been given to the development and use of new hypoxia tracers over the past 40 years. Nakamura et al first discovered that a 5-nitroimidazole (azomycin) was active against infections in a hypoxic environment.[45] Nitroimidazoles undergo reductive metabolism in all tissues with viable enzymatic processes,

but retention in tissues occurs only when there is low oxygen tension. In these tissues, reoxidation of the original compound is slow, permitting further reduction to more reactive products that bind to cell components.[46] This unique behavior of nitroimidazoles in a low oxygen environment has led to investigations of their utility as hypoxic tissue tracers for more than 10 years.

Many nitroimidazole analogs have been synthesized and studied in *in vivo* and *in vitro* investigations.[5,45-50] N'-substituted 2-nitroimidazole derivatives, especially MISO (3) analogs have been the major agent investigated thus far. ^{14}C-ring labeled MISO (4) and ^{3}H-side-chain labeled MISO (5) were found to bind selectively to hypoxic cells *in vitro* in EMT-6 spheroids [51,52] and *in vivo* with Balb/c mice bearing EMT-6 tumors.[53,54] Autoradiographic techniques with ^{3}H- and ^{14}C-MISO were also employed to measure hypoxia in human tumors.[55,56] These early studies demonstrated the usefulness of radiolabeled MISO analogs as markers of tissue hypoxia. Although these β^{-} emitting MISO analogs are not suitable for non-invasive diagnosis, they did provide evidence that MISO analogs could be useful for *in vivo* detection of hypoxia when gamma-emitting or positron-emitting radionuclides were present. As a result, a number of brominated and fluorinated analogs of MISO were tested. The initial study with ^{82}Br-MISO (6) showed that it had some potential for imaging tumor hypoxia.[57] However, extensive *in vivo* debromination limited its

utility.[58] More recently, several other studies with ^{18}F-MISO (1) showed that these compounds had promise as non-invasive tracers of hypoxic cells in tumor and in ischemic brain areas.[6,59] The utility of ^{18}F-MISO is limited by the short half life of ^{18}F (110 min) as well as the requirement for on-site PET imaging capabilities.

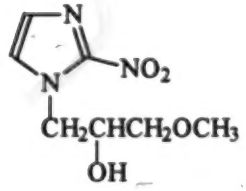

3

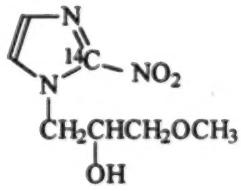

4

5

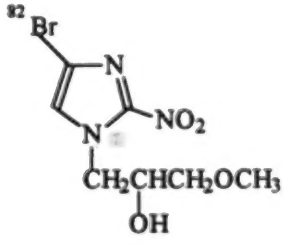

6

MISO was also tested in clinical trials as an hypoxia cell radiosensitizer. Clinical evaluation of this drug was disappointing due to its peripheral neurotoxicity at the therapeutic dose level.[60] This toxicity is relevant only to the high concentration of MISO (100-600 μM) that

is required for radiosensitization.[61] In comparison to this high concentration, the required concentration of radiolabeled MISO analogs for imaging studies in human is only about 1 μM.[62] Investigation with nitroimidazoles as hypoxic tissue imaging agents continued further in an effort to identify compounds having similar or better selective binding to hypoxic tissue with less toxicity than misonidazoles.

2.2.2. Metabolic Pathway of Nitroimidazoles

It has been demonstrated that nitroimidazoles are reduced intracellularly by nitroreductase in a variety of cells. In the absence of adequate supplies of oxygen, they undergo further bioreduction to more reactive products that bind to cellular components.[63-66]

The process of nitro-reduction predominantly occurs in liver,[67] hypoxic cells of tumors [68] and by intestinal microflora.[69] The detailed nitro-reduction process is shown in Scheme 2.1 adapted from Edwards.[63] In either aerobic or hypoxic cells, the reduction is initiated by an enzyme-mediated single-electron reduction of the nitro-group to a free radical anion.[63,70] In aerobic cells the intracellular oxygen (reduction potential of -155mv) has a higher electron affinity than the nitro group, thus resulting in reversal of the initial reduction with the regeneration of intact nitroimidazoles. This process inhibits further reduction of the free radical anion to more reduced products.[71,72] On the other hand, in hypoxic tissues where the O_2 concentration is low, the bioreduction pathway may proceed in successive steps through the hydroxylamine intermediate to terminate at

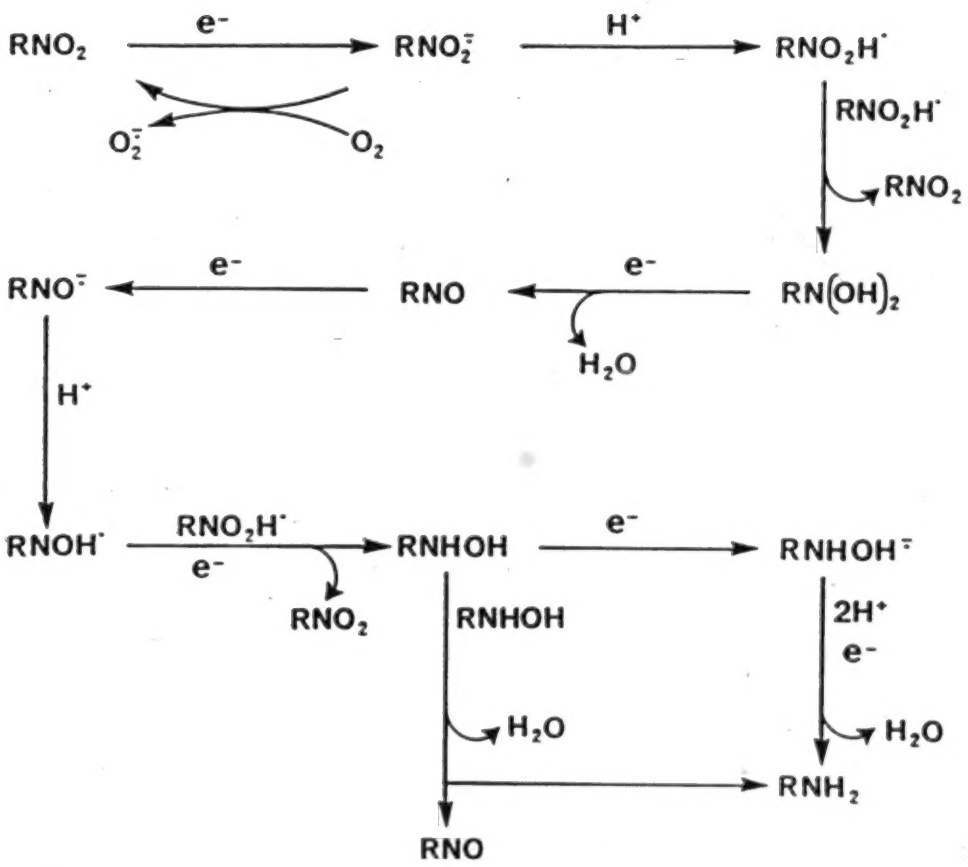

Scheme 2.1. Sequence of the reduction and electron transfer process in nitroimidazoles. (Adapted from Edwards [63])

the relative inactive fully reduced amine derivative.[63,70] In addition, this enzyme-mediated reduction will not occur in "dead" or infarcted tissues and thus has selectivity toward hypoxic tissues.

The amine derivative is believed to be relatively inert with respect to binding to cellular components. Therefore, the nitroso and hydroxylamine intermediates would appear to be the most active species as bioreduced metabolites from the nitroimidazole reduction pathway.[73] Studies also indicate that the hydroxylamine intermediate is mainly responsible for adduct formation with cellular macromolecules.[74,75] It is known that hydroxylamines are capable of reacting with a variety of biologically important molecules in chemical systems and that these reactions can be demonstrated in cell systems, in whole animals and in humans.[75] However, the cellular components that the reduced products react with have not been unequivocally identified. It has been reported that the products of the nitro-reduction pathway are capable of binding covalently to nucleic acids and proteins.[74,76] Raleigh et al demonstrated the importance of intracellular thiols in the reductive binding of 2-nitroimidazoles to cellular protein rather than DNA.[77] It is also noted that reduced 2-nitroimidazole binding was concentrated in the cytoplasm of cells of spontaneous canine tumors.[78] Therefore, cytoplasmic reduction of 2-nitroimidazole may occur with cellular proteins being the primary target for binding, and with the possible diffusion of these reactive intermediates into the nucleus for further binding to DNA.[78]

2.2.3. Development and Characteristics of Iodoazomycin Arabinoside

Research at the University of Alberta has focused on the development of 2-nitroimidazole derivatives that could be labeled with appropriate radionuclides to permit non-invasive imaging of hypoxic tissue. Towards this end a variety of iodinated misonidazole derivatives were synthesized and tested *in vitro* and *in vivo*. In 1986, Jette et al iodinated azomycin riboside (AZR) (7), a known radiosensitizer and sugar-containing homologue of misonidazole. The sugar moiety provided a target for iodination and yielded a product that was less lipophilic than a number of iodinated compounds investigated in earlier studies.[79] The resulting compound, IAZR (8), was more toxic *in vitro* and radiochemically less stable *in vivo* than misonidazole.[79] It was, however, shown to be better than misonidazole in terms of radiosensitization and selective binding to hypoxic cells *in vitro*.[8]

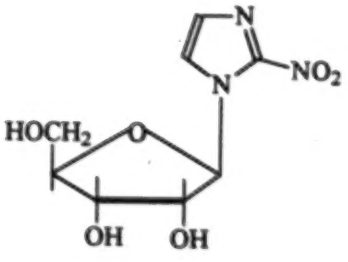

7

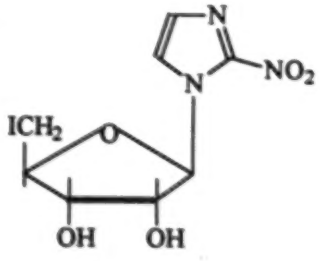

8

Because of these promising results, a series of analogs of IAZR were developed and studied both *in vivo* and *in vitro*[5,8] The most widely evaluated compound in this series is iodoazomycin arabinoside (IAZA) (2) which has undergone extensive investigation in hypoxic cell cultures,[8] in animal distribution studies [8,10] and in clinical trials in cancer patients.[10,11]

Table 2.1. Octanol-water partition coefficients for MISO and its analogs. (Adapted from Mannan[8])

compound	partition coefficient (P)
IAZR	2.1
IAZA	4.98
MISO	0.43
4-Br-MISO	2.87
F-MISO	0.40

IAZA is an isomer of IAZR with higher lipophilicity than IAZR and MISO (Table 2.1). The higher lipophilicity is probably due to the substitution of the hydroxyl group by an iodo group at the 5' position of the sugar moiety.[8] In *in vitro* studies, ^{125}I labeled IAZA showed a hypoxia-dependent binding rate in EMT-6 cells more than three times that of MISO.[8] Although the elevated binding was accompanied by greater cytotoxicity than observed for MISO, IAZA was shown to be non-toxic to Balb/c mice bearing EMT-6 tumors at

a dosage 100 to 120 times greater than the human dose anticipated for *in vivo* scintigraphic studies. This suggests that IAZA could be used for scintigraphic studies in human subjects without any toxicity. On the other hand, the biodistribution studies in Balb/c mice bearing EMT-6 tumors showed a rapid excretion (>98% in 24 hours) of ^{125}I-IAZA. Excretion was predominantly by the renal route with some involvement of the hepatobiliary route.

The tumor radioactivity, in terms of percent of injected dose per gram and in terms of tumor-to-blood ratio, was found to be higher than in any organ with the exception of thyroid at time periods between 4 and 24 hr. The tumor-to-blood ratios reached a maximum of 8.7 at 8 hr post injection and dropped to 5.8 at 24 hr.[8] These higher selective binding ratios made IAZA a more suitable compound for non-invasive detection of hypoxic tissue than a number of other previously studied iodinated 2-nitroimidazole analogs. Furthermore, iodine-123 labeled IAZA enables the measurement of this hypoxic marker by both planar scintigraphy and SPECT using nuclear medicine equipment available in most hospitals.

Indirect evidence from clinical studies has suggested that chronic cellular hypoxia affects the radiocurability of some human tumors. Therefore, the development of non-invasive assays of tumor oxyge-

nation status will be very helpful in predicting the prognosis of patients receiving radiotherapy.[10] In preliminary clinical trials in cancer patients, the uptake of ^{123}I-IAZA into tumors was correlated with a deficit in blood flow to those tissues as indicated by ^{99m}Tc-HMPAO.[11] This correlation suggests that ^{123}I-IAZA or related compounds could indicate the hypoxic status of a patient's tumors and thereby assist in the selection of treatment.

More recently, IAZA was explored in diabetic patients with peripheral vasculature insufficiency. A correlation existed between the transcutaneous oxygen tension ($TcPO_2$) chest/foot index and the degree of diffuse uptake of ^{123}I-IAZA.[81] Acute assessment of tissue oxygenation status in diabetic patients is expected to have significance in the diagnosis and treatment of limb complications secondary to impaired microvasculature. It may also indicate tissue at risk of impending ulceration and predict the success or failure of ulcer or wound healing.

The promising results obtained with IAZA in evaluation hypoxic tissues have led us to employ this compound in the present stroke study. This thesis will report new biological and biodistribution data used to evaluate the potential of IAZA as a non-invasive tracer of brain ischemia in stroke patients.

2.2.4. Hypoxic Tracer Studies in Animal Stroke Models

Because of their unique hypoxia-selective binding properties, MISO and its analogs have been investigated recently in stroke studies. ^{3}H-MISO was tested in gerbils subjected to unilateral artery occlusion. The hemispherical uptake of this agent occurred only in the ipsilateral brain sections and was correlated positively with the severity of brain damage as measured by stroke index (SI).[82,83] The autoradiographic results also suggested that the intense uptake of ^{3}H-MISO (5) in brain tissue is not due to the diminished blood flow retarding its washout, but most likely due to its covalent binding in hypoxic tissues. However, ^{3}H-MISO is not suitable for imaging and human studies. Other tracers labeled with gamma-emitting or positron emitting radionuclides, however, appear to have potential as imaging agents for hypoxic/ischemic tissue. One such compound, a ^{99m}Tc labeled complex of 2-nitroimidazole (BMS-18132) (9) was examined in a rat stroke model.

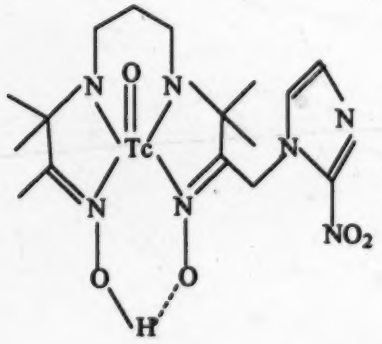

9

Autoradiograms of the brain showed this complex was retained in ischemic tissue at risk of infarction, but was not retained in already infarcted tissue.[44] The distribution of activity also indicated the presence of a penumbra effect with uptake at the outer ischemic tissue surrounding an infarcted core with no uptake. Analogs of MISO have also been radiolabeled with fluorine-18, a positron-emitting radionuclide. Studies in the gerbil model showed that the selective uptake of ^{18}F-MISO (1) was dependent on the extent of hypoxia in the brain tissue.[6] A further preliminary clinical trial also reported that three of six acute stroke patients had intense uptake of ^{18}F-MISO in the ischemic penumbra, but patients with chronic infarction had no ^{18}F-MISO retention.[7] Unfortunately, ^{18}F labeled markers are only available in those facilities with cyclotron and positron emission tomography instrumentation, and their use is further limited by the relatively short half life of ^{18}F (110 min).

2.3 STROKE ANIMAL MODEL

2.3.1 Brain Vasculature of the Mongolian Gerbil

A variety of animal species, ranging in size from small rodents to large subhuman primates, have been used in stroke studies. However, large species such as dogs and non-human primates are not only very expensive but also unacceptable for ethical reasons. More important, ligation of cervical arteries does not induce

significant changes in brain circulation of most species. This is because in most species there are numerous end-to-end anastomoses that establish connections between branches of the internal and external carotid arteries.[84,85]

In 1969, the Mongolian gerbil was introduced into stroke study because of its unique brain vasculature.[85] Levine and associates first analyzed the anatomy of blood vessels in gerbils and found no significant connections between the basilar-vertebral system and the carotid system.[86] Subsequent anatomy studies confirmed the absence of the expected posterior communicating arteries (PCOA) and demonstrated the detailed of the brain vasculture in the Mongolian gerbils.[57-59]

The scheme of blood vessels supplying the gerbil brain is shown in Figures 2.1and 2.2 adapted from Mayevsky.[90] The common carotid artery system and the vertebral artery system are the two sources supplying brain circulation. The internal carotid artery rises from the common carotid artery and has three main branches supplying various parts of the cerebral hemisphere, namely the anterior, middle and posterior cerebral arteries (ACA, MCA and PCA), respectively. On the other hand, the two vertebral arteries form the basilar artery which itself is divided into the superior cerebellar arteries (SCeA) supplying the cerebellum. In 80-90% of the Mongolian gerbils, there is a lack of connecting arteries (PCOA) between the two circulation systems.[91] This anatomy feature renders the Mongolian gerbil

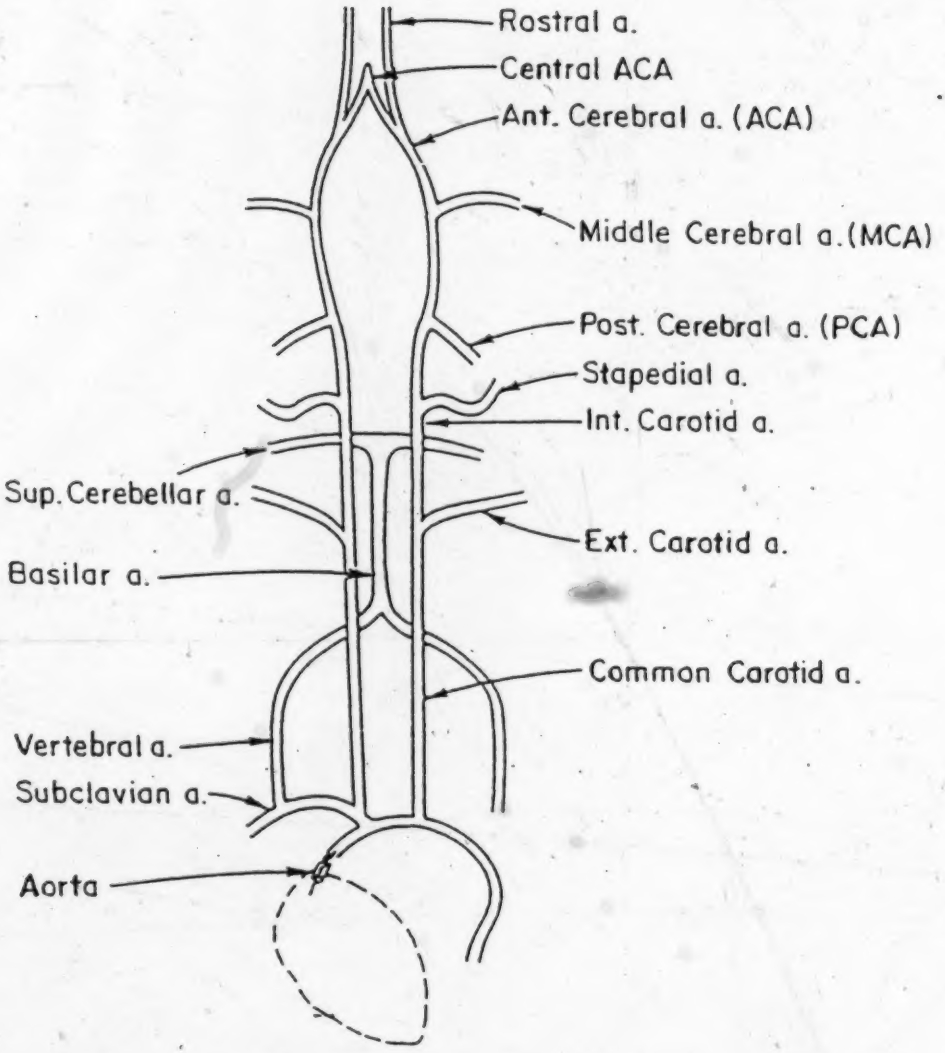

Figure 2.1. General schematic presentation of blood vessels originating from the aorta and supplying the gerbil head and brain. (Adapted from Mayevsky [90])

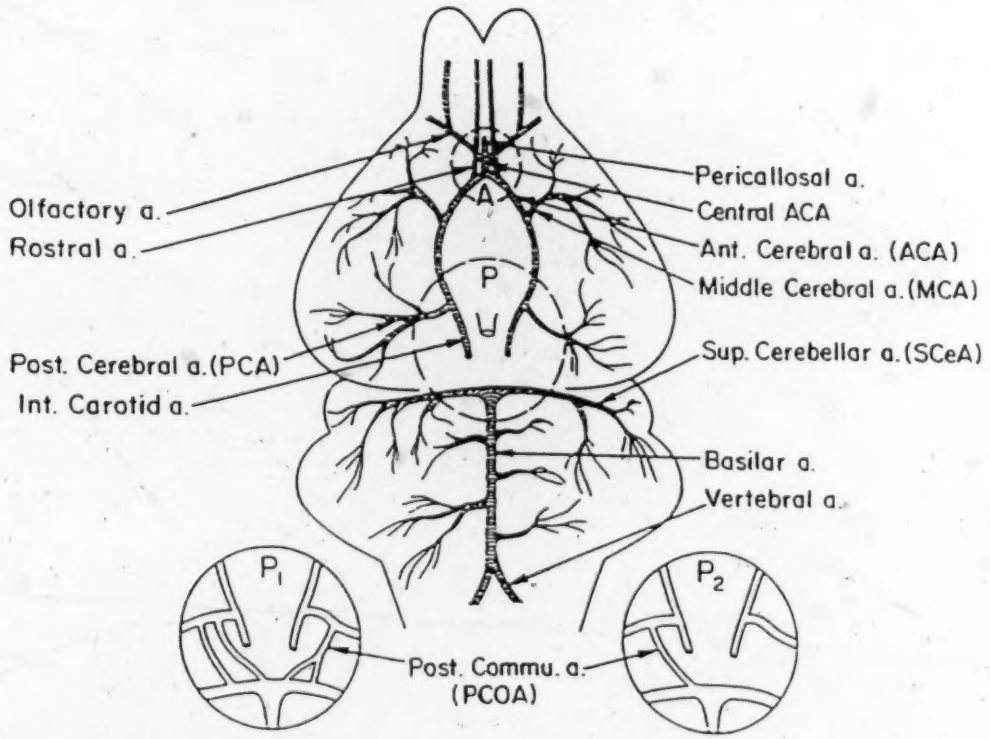

Figure 2.2. Detailed presentation of the two sources of blood vessels reaching the brain in the Mongolian gerbil. (Adapted from Mayevsky [90])

susceptible to forebrain ischemia following common carotid artery occlusion. Although the PCOA may exit in 3-20% of the gerbils, the actual level of ischemia was close to 100% in all gerbils that were exposed to bilateral carotid ligation. This may due to the secondary vasoconstriction response to the ischemia.[92,93]

2.3.2 Common Carotid Artery Occlusion

The methods of inducing ischemia determines the results of experiments in the gerbil stroke model. There are two methods used in this animal model to induce cerebral ischemia: unilateral carotid artery occlusion (UCO) and bilateral carotid artery occlusion (BCO).

In Levine's study, 20% of the gerbils had severe neurological symptoms and died within 2 days after they were subjected to unilateral carotid artery occlusion.[85] Numerous other studies have claimed the susceptibility of this species to develop severe neurological signs and unilateral hemisphere infarction in about 30% to 60% of cases following unilateral carotid artery occlusion.[87,88] However, because of the high percentage of mortality which occurs within few days after unilateral ligation, and the low incidence of brain ischemia in the surviving animals, the bilateral occlusion method appears to be gaining favor over the unilateral occlusion method.

In the bilateral occlusion method both carotid arteries are transiently

occluded and followed by reperfusion. The occlusion is allowed to proceed for the length of time appropriate for the particular investigation. Since the gerbils lack PCOA between the vertebral circulation and carotid circulation, it is easy to induce high-grade bilateral forebrain ischemia by simply ligating the two carotid arteries in the neck. Experiments using the hydrogen clearance CBF techniques have shown that forebrain blood flow falls to near zero during ligation in most gerbils, with some gerbils having a residual flow of about 0.1ml/gm/min.[94,95] It is reported that as little as 5min of bilateral ligation could cause typical hippocampal lesions in about 90% of gerbils.[96] Following longer ligation (20-30 minutes), similar damage was seen in more rapid and severe forms.[97] Principally because of its convenience, the bilateral occlusion method has been applied broadly in studies of patho-physiology, morphology and pharmacoprotection.

2.3.3. Cerebral Blood Flow and Metabolism Following Ischemia

Under normal conditions, an increase in brain metabolism would induce a proportionate increase in brain blood flow. In the post-ischemia period, however, discrepancies between blood flow and metabolism may occur that could be important in the development of brain damage and may also affect response to treatment.

A variety of studies have delineated the dynamics of regional blood

flow and metabolism in post-ischemia brain. Figure 2.3 shows cerebral blood flow and metabolism changes during and after ischemia as proposed by Siesjo.[97] A short-lasting cerebral hyperemia has been noted after restoration of blood flow in different animal models. This reactive hyperemia is probably the result of ischemia-induced accumulation of extracellular hydrogen ion (H^+) through lactic acid formation[98] and efflux of potassium ion (K^+) from intracellular pools.[99] Both ions are known to relax cerebro-vascular smooth muscle.[100] On the other hand, since the concentration of adenosine triphosphate (ATP) is depleted during the ischemia period, the expected secondary accumulation of adenosine, a potent cerebral vasodilator, may also play a role in mediating the initial hyperemic response.[101]

However, whether the ischemia is completed or incomplete, resto-ration of an adequate perfusion pressure normally leads to a delayed hypoperfusion following reactive hyperemia within one hour of reperfusion.[102-105] In gerbils subjected to one hour unilateral ligation, both ipsilateral and contralateral CBF fell and remained below normal for at least 4 hours after recirculation.[102] A decreased CBF was also observed by 10 minutes after reperfusion and this flow returned to a normal level at 6 hours in gerbils subjected to 5 minutes bilateral occlusion.[103] Similar hypoperfusion has been demonstrated in other animal models during the post-ischemia period.[104-106]

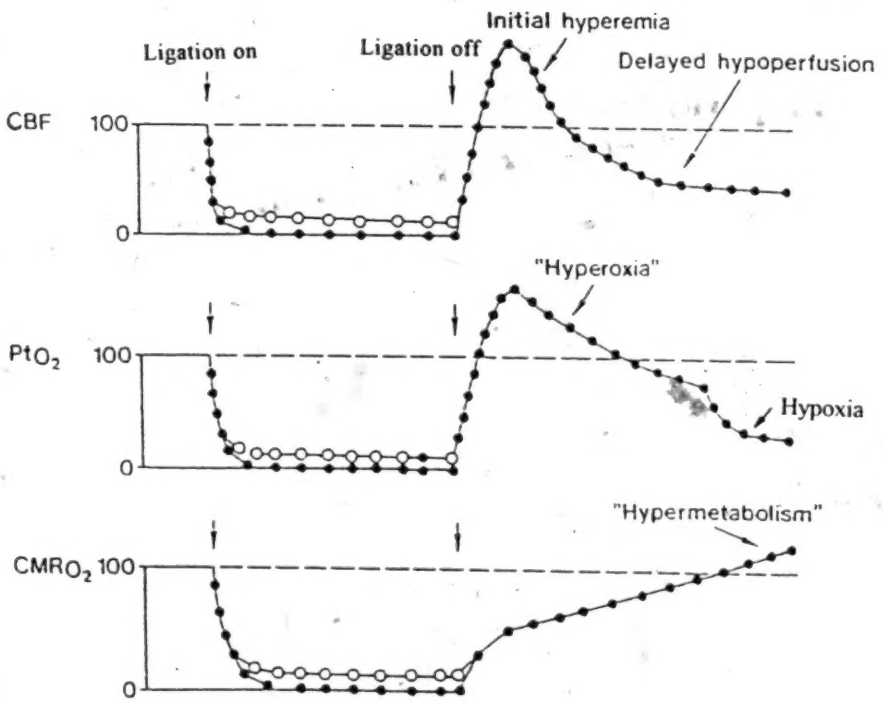

Figure 2.3. Schematic diagram illustrating changes in CBF, tissue PO_2 and $CMRO_2$ during ischemia and in the recirculation period. Filled circles: complete ischemia; open circles: incomplete ischemia. (Adapted from Siesjo [97])

Mechanisms proposed to explain delayed hypoperfusion include physical compression or blockage of vascular lumen[107] and increased vascular smooth muscle tone.[108] However, vascular occlusion by mechanical factors, such as endothelial swelling and aggregation of platelets or red blood cells, seems an unlikely explanation for post-ischemia hypoperfusion. No indication of accumulation of the above factors was found in animal studies.[103,109] Therefore, post-ischemia hypoperfusion probably results from increased vascular smooth muscle tone[109,110] and in this respect release of vasoactive amines[111] and disturbance of calcium ion homeostasis in cerebrovascular smooth muscle could contribute to post-ischemia vasoconstriction.[99]

In post-ischemia brain, depression of metabolism is expected to accompany decreased CBF. However, many investigators have demonstrated increased metabolism in the post-ischemia period. A marked imbalance in decreased CBF and high-energy phosphate metabolism occurs during the post-ischemia period and was most pronounced after 4 hours.[102] Further demonstrations of an uncoupling between CBF and metabolism were shown by increased local cerebral glucose utilization (LCGU) and $CMRO_2$, accompanied by perfusion deficits after several hours of recirculation.[103,112] These high metabolic demands of the electrically active brain[113] under the low CBF state may cause a misrelating between oxygen demands and availability, resulting in a relative tissue hypoxia in the brain.

2.3.4. Changes in Blood-Brain Barrier Following Ischemia

Though the factors involved in the breakdown of blood-brain barrier (BBB) are not completely understood, several studies have investigated the pattern of BBB impairment during reperfusion in gerbils.[103,114,115]

Two separate openings of the BBB were observed in gerbils subjected to bilateral ligation.[84,103] The first one occurred shortly after reperfusion and might relate to the hemodynamic effect of greatly increased intraluminar pressure in blood vessels.[103] However, other studies reported that the barrier in gerbils remained largely intact up to 17 hours after ligation.[83,84] The second opening was noted several hours to days later. It appeared to be independent of CBF changes and was associated with severe neuronal damage in hippocampal CA1 sector. This opening maybe due to the release of some compounds from neuronal elements damaged by ischemia, which would stimulate pinocytotic activity in the vascular endothelium.[103] Other studies also indicated that BBB breakdown was related to the length of ischemia. It took 20 hours delay for the development of the BBB lesion in 50% of the gerbils occluded for 30 minutes. However, with 6 hours occlusion, 100% of the gerbils showed BBB breakdown within 1 hour after release of ligation.[114,115]

Two types of edema; vasogenic and cytotoxic, the former related to extracellular and the latter to intracellular edema; have been

attributed to failure of the BBB. The cytotoxic edema develops during ischemia and shortly after restoration of blood flow, while vasogenic edema appears as a later event within hours or days after the cytotoxic edema has been resolved.[114-116] In cytotoxic edema, parenchymal structural elements are directly affected by noxious factors, resulting in intracellular swelling. In vasogenic edema, the increase in water content is accompanied by passage of serum protein from the blood into the brain. This type of edema is related to BBB damage which facilitates an escape of water and plasma constituents into adjacent parenchyma.[116]

2.3.5. Factors Affecting Brain Ischemia

It is believed that the brain temperature is the single most important factor that influences ischemic damage in the gerbils. Several studies have observed that hippocampal pyramidal neurons of the CA1 layer showed moderate to severe histological damage in 100% of the hemisphere when brain temperature is held at 36°C during ischemia. However, histological damage occurred in only 20% of the hemispheres held at 34°C, and in 0% of the hemispheres held at 32-33°C. Similar ischemic injury to other selectively vulnerable zones was reduced by approximately 80% at 33-34°C.[117] It is known that hippocampal damage is due to an excessive accumulation of intracellular calcium precipitated by elevated levels of

glutamate during ischemia.[118] Mild hypothermia (e.g. 29 -33°C) during or immediately after ischemia can significantly reduce the severity of ischemic insult, possibly as the result of attenuating the glutamate level.[119] This marked dependence of ischemic damage on brain temperature suggest that the failure to monitor or maintain brain temperature, or allowing body temperature to change during ischemia might introduce unacceptable variation into the results of experimental ischemia research. Other studies also demonstrate that brain temperature may vary independently of rectal or skull temperature, but temporal muscle temperature closely reflects brain temperature.[120,121] Therefore, in order to avoid the confounding effects of hypothermia, it is necessary to monitor and maintain the brain temperature during ischemia and the post-ischemia period.

Plasma glucose level is another factor that may affect ischemic insult. High plasma glucose has been shown by a number of investigators to exacerbate the effect of transient ischemia and of hypoxia in gerbils.[122,123] Hyperglycemia is known to be associated with decreased intracellular pH, increased brain lactic acid accumulation, impaired recovery of ATP and delayed recovery of CBF.[123-125] Therefore, overnight fasting of animals or monitoring of plasma glucose should be built into study design if precise control of ischemic damage is necessary.

Several agents including ether, nitrous oxide-oxygen mixtures,

halothane-oxygen mixtures and various barbiturates are used to provide anesthesia during artery occlusion.[126-128] Some caution should be exercised since experimental evidence indicates that some anesthetics may influence the extent or nature of ischemic injury. For example, nitrous oxide produces anesthesia by inducing generalized anoxia, which may alter the consequences of ischemia. Barbiturates, on the other hand, reportedly protect tissue against the deleterious effects of ischemia.[126,127] Consequently, the choice of anesthetic is important in the proper design and control of animal studies.

The age of animals is also a factor that must be taken into account in study of brain ischemia. Infant and young gerbils have been found to be resistant to cerebral infarction following carotid artery ligation. It is conceivable that younger gerbils have a highly developed network of collateral blood vessels between vertebral and carotid systems.[128,129] However, gerbils can be a suitable model for stroke research when they are 5 weeks old or older.[128,129]

2.4. AUTORADIOGRAPHY

2.4.1. The Principle of Autoradiography

Radiography allows visualization of the patterns of distribution of radiation. In general, autoradiography is the localization within a

solid specimen of radiolabel determined by placing the specimen against a layer of recording medium, as shown in Figure 2.4.

Figure 2.4. Generalized schematic diagram showing vertical section through an autoradiograph.

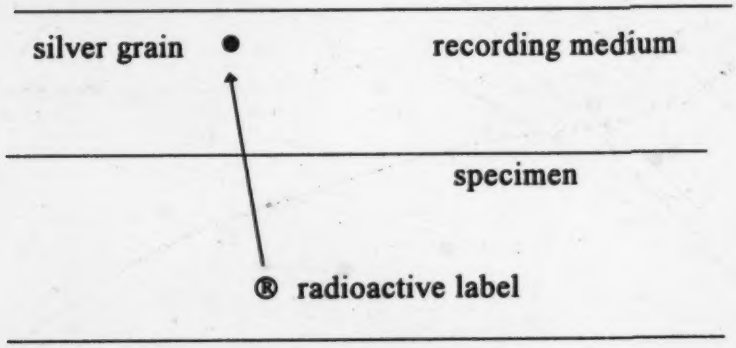

The principle of the autoradiography process is that radioactive decay taking place within the specimen emits particles of radiation (β^-,e^-) which, after suitable exposure time, produce a useful number changes in the medium layer. The pattern or position of these changes in the medium will correspond in some way to the original activity in the sample. These alterations within the medium are then amplified in such a way as to make them visible with or without aid to the naked eye.[130] In autoradiography, the specimen itself is the source of the radiation. The recording medium which gives rise to the resultant image is either photographic emulsions or nuclear emulsions. These emulsions are generally crystalline silver halide mixtures (AgI, AgCl, AgBr) dispersed in gelatin. When the emulsion

is exposed to light photons, X-rays or moving charged particles, the Ag^+ ions are reduced to atomic silver resulting in the formation of metallic silver in those crystals.[130] In the process of amplification, the size of the metallic silver deposited will be increased until it reaches a threshold at which it can be recognized. At this threshold, the crystals become silver grains which can be visualized often with the aid of a microscope.[130]

2.4.2. Components of Autoradiography

2.4.2.1 Specimen

Many types of specimen can be studied by autoradiography. In light microscope autoradiography, 4-6 μm thick specimens are often used. The emphasis is on minimizing exposure time while retaining adequate histological quality. In order to cut suitably thin specimens, the tissue must have a certain hardness and uniformity. One way of achieving this is by dehydrating the tissue with alcohol and impregnating it uniformly with paraffin wax.[130]

2.4.2.2. Emulsion

Belanger and Leblond pioneered the use of liquid emulsion in order to achieve very close contact between specimen and emulsion.[130] Since then, many kinds of liquid emulsion have been developed and are available in a range of sensitivity and of grain sizes.

For studies of the localization of radioactivity within tissues, it is suggested that one use the liquid emulsion instead of stripping film. It is usually possible to obtain better resolution without any significant decrease in efficiency by using liquid emulsion rather than stripping film. Also, technically the process of dipping in liquid emulsion is very quick and simple, and adhesion of emulsion to specimen is better.[130]

It is apparent that increasing emulsion thickness increases grain density where β-particle range is greater than the emulsion thickness. Therefore, when working with tritium or isotopes emitting low energy electrons (^{125}I), the emulsion layer should be 3-4 μm, which is thicker than the maximum track of the isotope, in order to absorb all particles entering the emulsion layer.[130]

2.4.2.3. Radioisotopes

The choice of radioisotope for a particular experiment will depend on two important factors: its biological relevance and the nature of the radiation emitted.

It is known that the higher the energy of a particle, the further it is likely to penetrate through a specimen and emulsion. Therefore, tritium with mean energy of 5.5 KeV and carbon-14 with mean energy of 50 KeV, are the most extensively used owing to their low emitted energy and the ease with which they can be incorporated

into almost any organic molecule. Both radionuclides are beta emitters which produce particles of nuclear origin given off as a continuous spectrum of energies up to maximum (Emax) of 18 KeV for ^{3}H and 156 KeV for ^{14}C.[130]

Iodine-125 emits Auger electrons at very low initial energies (0.8-2.9 KeV), in the range of those beta particles emitted by tritium. It thus shares with tritium the advantage of giving very good resolution in most autoradiographic systems. Iodine-125 decays by electron capture producing low energy X-rays and γ-rays as primary emission and energetic electrons as a secondary emission during stabilization of electronic energy levels following decay. The Auger electrons are produced as discrete line spectra and are important for production of the silver grains at the light microscopic level of autoradiography.[130]

2.4.3. Autoradiography in the Evaluation of Stroke

Autoradiographic research of brain function began in late 1950s. Since then, autoradiography has been widely applied in the investigation of blood flow and metabolism studies.[131-133] Several autoradiographic studies have also been performed to measure hypoxic tracer distribution in animals.[44,82,83] For example, both ^{3}H and ^{99m}Tc labeled MISO analogs were investigated to detect brain ischemia in animal stroke models. The results of these studies indicate that the

autoradiographic technique is a useful method to localize the *in vivo* distribution of radiolabeled hypoxia tracers.

Light microscope autoradiography was used in the present study to observe the biodistribution of radiolabeled IAZA in both ischemic and non-ischemic brain tissues.

3. EXPERIMENTAL

3.1 MATERIALS

3.1.1 Chemicals, Solvent and Equipment

All chemicals used were reagent grade unless otherwise specified. Gases were purchased from Praxair Inc., Canada and were of research purity. Thin layer chromatography (TLC) was performed on silica gel Kieselgel 60F plastic sheets. Radiochemical syntheses were carried out in Pierce React-vials™ capped with Mininert valves, with heating by a Baxter Multi-block Module heater. Eppendorf micropipettes were used for measuring micro quantities of solvent.

3.1.2. Instruments

Tissue samples and TLC microplates containing ^{125}I were counted in Beckman Gamma 8000 gamma scintillation counter. A Fisher microtome was employed for cutting tissue samples. A Leitz light microscope was used for observing autoradiograms and collecting data.

3.1.3. Anesthetics and Surgical Tools

Xylocaine was purchased from Health Science Laboratory Animal Service, University of Alberta. Halothane and surgical tools, such

as blades, scissors and needles were purchased from the Surgical-Medical Research Institute, University of Alberta. All surgical tools were sterilized before being used. A Ohmeda halothane apparatus was used for anesthetizing animals. A microprobe needle and a Marnant 100 thermometer were used to monitor brain temperature via implant in the temporal muscle.

3.1.4. Materials Used in Autoradiography

Kodak autoradiography liquid emulsion, Kodak developer D-19, Kodak Polymax fixer and stop bath were purchased from Eastman Kodak company, U.S.A.. All these solutions were diluted before being used. Hematoxalin and Eosin stain solution were purchased from BDH Inc., Canada. Tissue sections were mounted on Fisher microscope slides.

3.1.5. Radioisotope

^{125}I was purchased from Amersham International, Canada. The radioisotope was purchased in the standard commercial form as no-carrier-added solutions of NaI in 0.1N NaOH.

3.1.6. Animals

Male/female adult Mongolian gerbils 40-50g were purchased from Charles River Canada Ltd. through the Health Sciences Small

Animal Program, University of Alberta. All animals were maintained *ad libitum* with rodent food pellets and tap water in standard plastic cages.

3.2. METHODS

3.2.1. Synthesis of 1-(5-Iodo-5-deoxy-β-D-arabinofuranosyl)-2-nitroimidazole (Iodoazomysin Arabinoside: IAZA)

The title compound was synthesized by Dr. Piyush Kuman, Faculty of Pharmacy, University of Alberta. The detailed steps of this synthesis are described elsewhere.[7]

3.2.2. Radioiodination and Purification of IAZA

3.2.2.1. Pivalic Acid Melt Exchange Labeling

IAZA was radioiodinated using pivalic acid in a melt method.[5] Briefly, no-carrier-added ^{125}I-NaI (37-74MBq), supplied in 10-20 μL of 0.1N NaOH solution was evaporated to dryness by a stream of nitrogen over 30min. Pivalic acid (3mg) and a solution of IAZA (0.5-1.0 mg in 100μL of HPLC grade aqueous methanol) was added to the Reacti-vial, and the solution was again evaporated to dryness with a stream of nitrogen. The Reacti-vial was sealed and heated at 80°C for 75 min in a heating block. The contents of the vial were then allowed to cool and dissolved in 100 μL of HPLC grade

aqueous methanol. The radiochemical yield and purity of the crude reaction mixture were determined by TLC method.

3.2.2.2. Thin Layer Chromatography (TLC)

1.0 μL of the radiolabeled sample was spotted on a TLC plate and developed in 10% methanol (MeOH:$CHCl_3$ ≅ 10:90). The TLC plate was previously spotted with cold IAZA to increase the concentration of the sample and prevent non-specific binding of the very dilute radioactive samples. After the development of the TLC plate, it was observed under UV light and the IAZA position was marked on the plate. Then, the plate was cut into 10 fractions. All fractions were counted in the gamma counter and the results were used for calculating radiochemical yield.

3.2.2.3. Purification of ^{125}I-IAZA

Silica gel column chromatography was used to isolate and purify the radiolabeled compound. ^{125}I-IAZA was dissolved in 50-100 μL HPLC grade aqueous methanol and loaded onto a disposable pipette filled with silica gel. Then, additional 3-4 mL portions of 3% methanol (MeOH:$CHCl_3$ ≅ 3:97) were continuously loaded to the column and 30-50 fractions (1-1.5 mL) were collected in small glass vials. 1 μL of each fraction was then counted to determine the

relative activity in each vial. The fractions with higher amount of activity were analyzed for radiochemical purity using TLC method as described in section 3.2.2.2., and those fractions having the highest purity (>95%) were combined for animal studies.

3.2.3. Animal Study

3.2.3.1. Surgical Procedures for Inducing the Animal Model

(1) Adult Mongolian gerbils are kept in an air-conditioned (25 °C) room to acclimatize for minimum one week prior to the study. Food and water are allowed *ad libtium*.

(2) The gerbil is sedated in an induction chamber with 5% halothane. The sedated animal is removed from the chamber and placed on its back on an operating pad warmed by circulating water. A nose cone is provided with a mixed flow of O_2 (5 mL/min) and halothane of 1.5-2%. The muscles should be completely relaxed before and during all surgical manipulation.

(3) A microprobe needle is placed in the temporal muscle and additional heating is provided by a heating lamp if the brain temperature drops below 37^{o}C during the surgery.

(4) The neck is cleaned with cotton swab and a midline ventral incision is made about 1cm long on the neck. Both common carotid arteries (CCA) are exposed by dissecting muscles parallel to the trachea. Each CCA is gently freed from its surrounding tissues and vagus nerves.

(5) For the ligation group: The arteries are gently lifted and a latex band is passed under each artery. When the brain temperature remains stable at 37.0°C-37.5 °C for several minutes, both CCA are ligated by using small clips. Ligation is maintained for a set period as defined by the operational protocol and the degree of ischemia required.

(6) After the ligation period, the clips are removed from arteries. Local anesthetic (1% xylocaine) is applied to the wound and the incision is closed with 2-3 skin sutures. The gerbil is returned to a clean cage for recovery.

(7) For the control group: Animals are subjected to the same surgical procedures except no carotid artery occlusion is performed.

3.2.3.2. Brain Temperature and Stroke Index Monitoring

A needle temperature probe is implanted in the temporal muscle to monitor the brain temperature in all gerbils. A thermometer is used to record the brain temperature before, during and shortly after surgery. The following form is used to record the temperature data.

Table 3.1. Form used to record brain temperature (°C) in control and ligation groups.

Group	5 min before surgery	start of surgery	start of ligation	during ligation/ surgery	end of ligation/ surgery	5 min after surgery
control			———			
ligation						

The gerbils' recovery from anesthetic and ischemia are also monitored at 15 to 60 minute intervals for several hours. The gerbils usually showed some neurological signs, such as hair roughed up, obtunded, eye fixed open, ptosis, circling, seizure and coma. These signs are tabulated as the stroke index such that a higher score indicate a more severe stroke damage.[135] Morbidity and mortality are evaluated and scored by using modified McGraw's method shown in Table 3.2.[136]

Table 3.2. Form used to record neurological signs and stroke index.

Animal age: _____ Animal weight (gram): _____
Date of surgery: _____ Total IAZA injected: _____
Time of injection: _____ Time of sacrifice: _____

neurological signs	Stroke index	15 min	30 min	45 min	1hr	2 hr	3 hr	4 hr	5 hr
hair roughed up / tremor	1								
obtunded	1								
hypesthesia of ear	1								
head cocked	3								
eye fixed open	3								
ptosis	1								
splay out hind limb(s)	3								
circling	3								
seizures	3								
extreme weakness	6								
total score	25								

3.2.3.3. Administration of Radiopharmaceuticals

Radiolabeled compound was stored dry and frozen and was reconstituted with physiological saline just prior to injection. The approximate radioactivity in the vial was measured by an isotope dose calibrator and the appropriate dilution was made so that each gerbil would receive the required activity in about 0.1 mL. For the biodistribution studies, the radioactivity present in 0.1 mL solution was 51.8-129.5KBq (1.4-3.5 μCi); for brain section studies it was 803-977 KBq (21.7-26.4 μCi); and for autoradiography studies, it was 1.84-5.08MBq (49.6-137.2 μCi). One to two hours after surgery, reconstituted radiopharmaceuticals were injected via the surgically exposed femoral vein in a single bolus injection with animals maintained under light halothane anesthesia.

3.2.3.4. Collection of Tissue Samples

Tissue samples of the gerbil that received injection of the compound were collected by the following procedures:

The gerbils were sacrificed by asphyxiation with carbon dioxide, followed by cardiac puncture. In biodistribution studies, in addition to the blood, other samples recovered were heart, lung, liver, kidney, spleen, small intestine, stomach, muscle, skin, bone, tail, thyroid and brain. Entire organs of the above samples were

dissected and collected into plastic vials and weighed wet using a taring balance. Stomach and small intestine samples were emptied of their food contents. Other organs were blotted to remove surface blood contamination. The muscle sample was removed from the upper hind leg, and the femur of this leg was removed as a sample of bone. A skin sample containing fur was taken from the upper back. The thyroid was collected with trachea and surrounding tissue. The brain was removed from the skull and the remaining carcass was divided into three portions. In brain section studies, following cardiac puncture, only the brain was removed and placed on dry ice for a few minutes. Then the brain was cut into slices of approximately 1.5-2 mm thickness, yielding a total of 7 coronal sections.

3.2.3.5. Counting and Analysis of Samples

All tissue samples containing ^{125}I were counted in a Beckman Gamma 8000 gamma scintillation counter. The decay per minute value (dpm) for each sample was determined in the preset ^{125}I counting window, with the correction for background. The dpm of the compound administrated to each animal was determined by counting a known volume of diluted injected dose. The dpm values were used for all calculation. The data from these samples at each time period and group were analyzed with the help of a computational data base program (Quatro Pro).

3.2.4. Autoradiography Study

3.2.4.1. Sample Preparation

The surgical procedures and administration of radiopharmaceuticals are described in section 3.2.3.1 and 3.2.3.3.. Five to six hours after injecting of ^{125}I-IAZA, the gerbils were sacrificed by asphyxiation with carbon dioxide. The whole brain tissue and a lobe of liver were removed and put into 10% formalin at room temperature for 5-7 days.

3.2.4.2. Tissue Processing

The brain and liver samples were removed from the formalin and dehydrated in xylene and increasing concentration of ethyl alcohol (EtOH) as shown below in Table 3.3. Then they were impregnated with paraffin wax and cut serially into coronal slices of 4um thickness using a Fisher Microtome. Finally, the sections were splayed on a water bath and mounted on microscope slides.

Table 3.3. Procedures for tissue dehydration.

Solvent	Time (minutes)	Frequency
70% EtOH	30	3
80% EtOH	30	2
95% EtOH	30	2
100% EtOH	30	2
Xylene	20	1
Xylene	45	1

3.2.4.3. Dipping and Development of Slides

Before dipping the slides, they were dewaxed through xylene and a descending series of ethanol alcohol concentration. Then, the slides were transferred to a dark room and dipped into diluted Kodak liquid emulsion (1:1 with H_2O). The slides were left in the cold plates for few minutes in order to gel the emulsion. They were transferred into drying boxes for several hours and wrapped with aluminum foil, then they were placed into cans with silica gel. Finally, the cans were again wrapped with foil and transferred to the refrigerator. In order to reach a balance between the fading of the latent imaging and the rate of disintegration of ^{125}I, the slides were exposed in liquid emulsion for six weeks. Six weeks later, the slides were developed by using standard developer, stop bath and fixer solutions.

3.2.4.4. Hematoxalin and Eosin Staining

After developing, the slides were first stained with Harris Hematoxalin for 5 minutes. Then, the slides were placed in PBS solution with LiO_3 followed by washing in cold running water for 5 minutes. Finally, the slides were stained with Eosin solution for 2 minutes and rinsed with ethyl alcohol solvents and distilled water. The slides were left to dry for a while and then observed under a light microscope.

3.2.4.5. Data Collection from Autoradiograms

All slides were observed under a Leitz light microscope. A grid in the eye-piece with 100 smaller squares (10um×10um) was used to count silver grains. The number of silver grains visible in the grid (1 mm^2) in different anatomic brain regions was recorded from a central brain section on a slide. The background was obtained by counting the silver grains outside the brain tissue section on a slide. For example, the silver grains were counted in cortex, hippocampus, thalamus, caudoputamen, etc.. The data was calculated as number of silver grains per grid with the correction for background. Silver grain distribution over different brain sections and anatomic sites were compared between the control and ligation groups.

3.3. STATISTIC ANALYSIS

In general, values are given as mean ± SD. Statistical significance of difference between the control and ligation groups was tested by two-sided t test for independent values. One-way analysis of variance (ANOVA) and Bonferroni multiple comparisons procedures were used for statistical comparison of significant differences among the ligation groups. Significant differences were considered to be present with a 5% level of confidence or better(see details in Appendices).

4. RESULTS AND DISCUSSION

4.1. Chemistry

Iodoazomycin arabinoside (IAZA) was synthesized by general procedures as described in detail elsewhere.[5] Radioiodinated IAZA (^{125}I-IAZA) was synthesized by exchange labeling using the pivalic acid melt method as show in Scheme 4.1. The reaction was complete in 75 minutes at 80°C.

Scheme 4.1. Radiolabeling of iodoazomycin arabinoside.

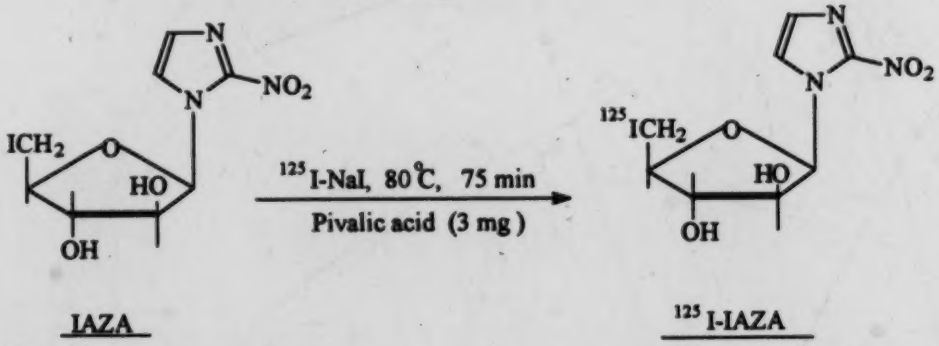

The radiochemical yield of crude products was determined by TLC as described in section 3.2.2.2.. Figure 4.1 shows a typical TLC chromatogram of a crude ^{125}I-IAZA sample. The radiochemical yield was then calculated using a computation data base program, based on the amount of radioiodinated product (IAZA) and free iodine on TLC plates as demonstrated in Figure 4.2 and Table 4.1. Our experiments showed a radiochemical yield of 80.07%-93.88% which was higher than previously reported.[5]

Figure 4.1. TLC chromatogram of ^{125}I-IAZA sample #96-08.

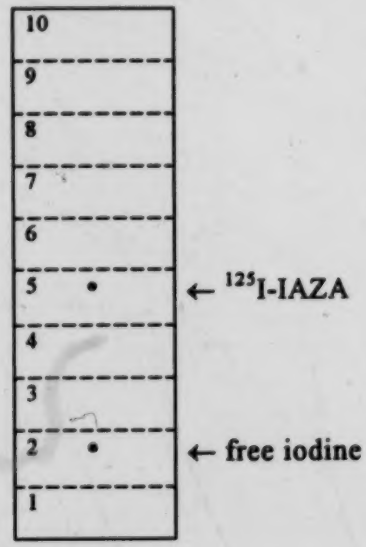

Figure 4.2. Diagram showing radiochemical yield of ^{125}I-IAZA sample #96-08 by plotting % total activity vs fractions.

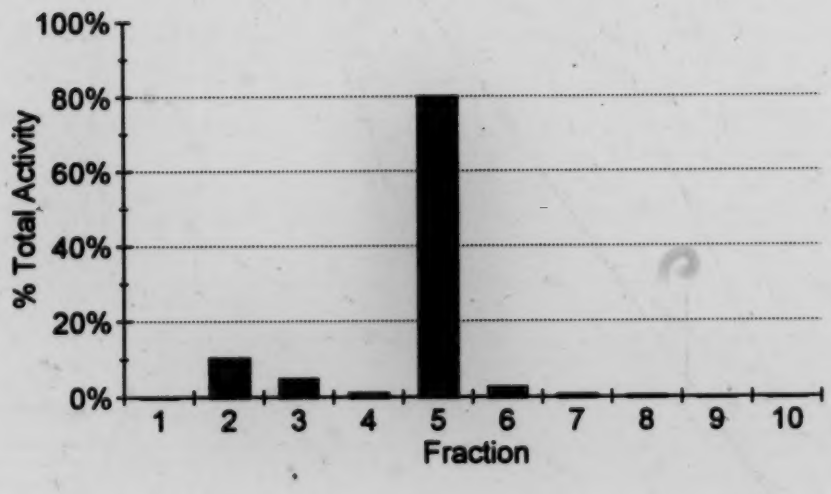

Table 4.1. Dpm values and % total activity of 10 TLC fractions of ^{125}I-IAZA sample #96-08.

Fraction	Dpm	Dpm-Bkg	% Total
1	405	149	0.03%
2	48749	48493	10.36%
3	22862	22606	4.83%
4	5254	4998	1.07%
5	375102	374846	80.07%
6	12485	12229	2.61%
7	3274	3018	0.64%
8	1587	1331	0.28%
9	569	313	0.07%
10	402	146	0.03%
Bkg	256		
Total		466039	100.00%

The radiolabeled product was then purified using silica gel column chromatography as described in section 3.2.2.3.. Figure 4.3 shows percentage of total activity vs fractions of ^{125}I-IAZA #96-08 after it was purified through column chromatography. The radiochemical purity of those factions with high amounts of activity (e.g. fractions 6-9) was determined by the TLC method described above. Those fractions having the highest radiochemical purity (>95%) were combined and used for animal studies. The purified compound was stored dry and frozen. Table 4.2 lists labeling and purification results of several ^{125}I-IAZA samples used in our experiments.

Sample: 96-08 Radionuclide: I-125
Solvent: Chloroform : Methanol = 95:5
Date: Aug 2nd, 1996 Activity: 0.8mci

Fraction	Dpm	Dpm-Bkg	% Total
1	1089	572	0.05%
2	1657	1140	0.10%
3	1146	629	0.06%
4	12065	11548	1.05%
5	16413	15896	1.44%
6	238914	238397	21.65%
7	272590	272073	24.70%
8	152158	151641	13.77%
9	131716	131199	11.91%
10	50512	49995	4.54%
11	41270	40753	3.70%
12	34462	33945	3.08%
13	34535	34018	3.09%
14	32652	32135	2.92%
15	30384	29867	2.71%
16	25947	25430	2.31%
17	21277	20760	1.88%
18	17829	17312	1.57%
19	16350	15833	1.44%
20	9850	9333	0.85%
21	9779	9262	0.84%
22	10118	9601	0.87%
23	7363	7346	0.67%
24	6547	6030	0.55%
25	5177	4660	0.42%
26	5364	4847	0.44%
27	4400	3883	0.35%
28	5525	5008	0.45%
29	4599	4082	0.37%
30	4263	3746	0.34%
31	3738	3221	0.29%
32	3267	2750	0.25%
33	2673	2156	0.20%
34	2092	1575	0.14%
35	2160	1643	0.15%
36	1968	1451	0.13%
37	2070	1553	0.14%
38	1701	1184	0.11%
39	1565	1048	0.10%
40	1385	868	0.08%
Bkg	517		
Total		1101350	

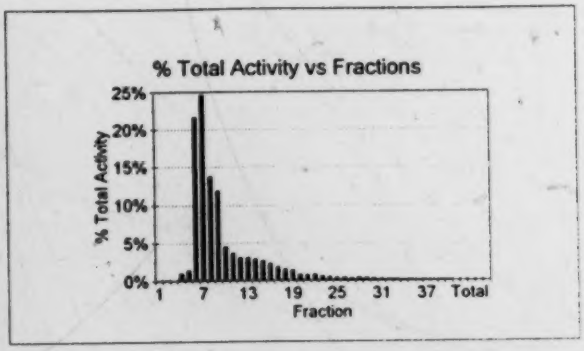

Figure 4.3. Percent of total activity vs fractions of [I-125]-IAZA #96-08.

Table 4.2. Results of IAZA labeling and purification.

Sample	^{125}I (mCi)	IAZA (mg)	Radiochemical Yield (%)[1]	Radiochemical Purity (%)[2]	Specific Activity (GBq/mmol)[3]
96-05	1.0	1.0	93.88	95.08	13
96-08	1.0	1.0	80.07	96.96	13
96-10	1.5	0.5	87.01	97.21	39

1. as determined for crude reaction mixture.
2. as determined following chromatographic purification.
3. as determined at the time of synthesis.

4.2. Observation During Surgery, Artery Occlusion and Recovery

Adult male/female gerbils (>6 weeks) were used in all animal experiments. Anesthesia induction required 3-5 minutes and was achieved by using 5% halothane in an insulated chamber. After induction of anesthesia, the gerbils were transferred to an operating table. A nose cone with a mixed flow of O_2 (5 mL/min) and halothane of 1.5-2% was used to provide anesthesia during surgery and ischemia. In order to avoid the neuroprotective effect of halothane anesthesia during the initial period of recirculation,[137] gerbils received no halothane after the clips were removed. Local anesthetic (1% xylocaine) was applied to provide anesthesia during wound closure. The muscles were completely relaxed during all surgical manipulation.

The surgery, artery occlusion and wound closure required 20-25 minutes (see details in section 3.2.3.1.). In the ligation group, all gerbils (n=36) that were subjected to 5 minutes of bilateral ligation showed a tendency to hyperventilate immediately after ligation. After release of ligation, they remained unconscious for 20-30 minutes. From 30 minutes to 4 hours post-ischemia, the gerbils showed some neurological signs such as splayed out hind limb(s), hair roughed-up, obtunded, eye fixed and open and ptosis. Circling was observed at irregular intervals for 1-2 hours after recovery in symptomatic gerbils. Seizure was only noted intermittently within 30 minutes post-ischemia in a few gerbils. After 4-6 hours recovery, some of the neurological signs, such as tremor and hair roughed-up, disappeared and the gerbils displayed normal running in cages. By 10-12 hours after ischemia, most gerbils in the ligation group could not be distinguished from those in the control group. All these symptoms were recorded and tabulated as stroke index to assess the severity of brain damage in ligated gerbils.

The control gerbils (n=18) were subjected to the same surgery procedures as ligated gerbils but without artery ligation. The control animals usually regained consciousness within 10-15 minutes after surgery. Most of them behaved normally after one hour of recovery. A few animals showed lack of digging movements which are common for normal gerbils.

Eight gerbils were also tested with 10 minutes of bilateral ligation. Seizure and abrupt explosive movement were observed in all gerbils shortly after release of ligation. Six gerbils showed continuous severe seizure and died within 2 hours. The other two gerbils showed similar seizure for 2 hours and remained in a semi-comatose condition for several hours until they were sacrificed. Though histological studies were not performed in our experiments, these observation indicate critical severe brain damage with this level of ischemia insult. Several histological reports have demonstrated that 4-5 minutes of bilateral ligation gives extensive necrosis of CA1 cells in the hippocampus in most gerbils and rats. Similar neuronal damage expands to the neocortical layer and caudoputemen in all animals after 8-10 minutes of ischemia.[96,103,109,138]

4.3. Brain Temperature Changes

It is believed that the outcome of brief ischemia is highly dependent on the brain temperature during and shortly after ischemia.[118,119] A reduction in brain temperature during ischemia and the first few minutes of recirculation can markedly reduce the severity of ischemic insult.[117-119] Therefore, we monitored and recorded the brain temperature in all animals. The gerbils were placed on a operating pad heated by circulating water (37°C) to maintain body and brain temperature. Additional heating was provided by a heating lamp if the brain temperature was below 37°C during surgery

and ischemia. The brain temperature was monitored by placing a needle temperature probe in the temporal muscle. This reading more closely reflects brain temperature than the reading of rectal or skull does.[120,121] The brain temperature recorded before, during and shortly after surgery are shown in Table 4.3.

Table 4.3. Mean±SD brain temperature (°C) in control and ligation groups.

Group	5 min before surgery	start of surgery	start of ligation	during ligation/ surgery	end of ligation/ surgery	5 min after surgery
control (n=18)	36.7±0.18	37.1±0.08	———	37.3±0.10	37.2±0.12	37.2±0.08
ligation (n=36)	37.0±0.16	37.2±0.20	37.3±0.11	37.3±0.13	37.8±0.10	38.6±0.33

The brain temperature in the control group did not show significant change and was maintained around 37°C during the whole surgical procedure. The brain temperature in the ligation group was kept about 37°C-37.5°C during the ligation period. However, the temperature showed a quick rise, which reached above 38°C shortly after release of ligation. Other studies reported a similar increase of brain temperature after surgical induction of ischemia.[139,140] This rise in brain temperature may introduce a pathological process that eventually leads to delayed neuronal death in the hippocampus.[139,140]

4.4. Biodistribution and Elimination

The *in vivo* biodistribution study of ^{125}I-IAZA was carried out in 24 gerbils. This study provided not only the distribution of radioactivity in different tissues at various time periods and the elimination of ^{125}I-IAZA, but also the distribution of radioactivity in ischemic and non-ischemic brain tissue in gerbils.

Numerous studies have demonstrated that 5min bilateral ligation could induce typical ischemic damage and significant CBF and metabolic changes in the brain of gerbils.[96,97,103,104] This method is also convenient, relatively easy to carry out by surgical techniques and results in very low mortality. In our studies, the gerbils were divided into two groups: in the ligation group, gerbils were subjected to 5 minutes of bilateral ligation; in the control group, gerbils were subjected to the same surgical procedures as the ligation group except for the absence of the ligation. All gerbils were allowed to have one to two hours recovery before they were injected with ^{125}I-IAZA. During this recovery period, we could monitor the gerbils' behaviors and neurological symptoms to evaluate the severity of brain damage as described in section 4.2.. One to six hours after induction of ischemia, a relative tissue hypoxia may exist in ligated gerbils due to a unbalance between the low CBF and hypermetabolism in the brain.[102-104]

One to two hours after surgical induction of ischemia, all animals were placed under light anesthesia (1.25-1.5% halothane in O_2 at 5 mL/min) and were injected with a single bolus of reconstituted ^{125}I-IAZA via surgically exposed femoral vein. The specific activity of the injected compound (^{125}I-IAZA) was 13.1 GBq/mmol. Each animal received an intravenous bolus dose of 51.8-129.5 KBq representing 1.4-3.5 μg of IAZA. The biodistribution results, as computed after measuring ^{125}I-IAZA activity in each organ and in the remaining carcass in both groups at various time periods, are shown in Table 4.4 and 4.5. No attempt was made to identify the metabolites or parent compound in these organs. Statistical significance of differences between the control and the ligation groups was analyzed by t test (see Appendix 1).

Table 4.4 and 4.5 reveal a rapid early distribution of ^{125}I-IAZA throughout the body with the brain containing the lowest radio-activity of all organs. At all 4 time intervals, the ligation group showed slightly higher level of activity in most organs than those of the control group, with the exception of lung and muscle which were slightly lower at one time interval. Hoffman et al reported similar findings after they evaluated ^{3}H-MISO in gerbils subjected to 5min of bilateral ligation.[83] Their results showed that the uptake of ^{3}H-MISO in non-CNS tissues (except liver) of the ligated gerbils were slightly higher than those of the control gerbils. However, there was no significant differences between the two groups.

Table 4.4. Biodistribution of ^{125}I-IAZA following i.v. administration in control groups with 2 hours recovery at various time intervals.

Tissue	Time (Hours) 2	4	8	24
Blood	0.2052±0.0033	0.1986±0.0154	0.1294±0.0009	0.0813±0.0064
Heart	0.0925±0.0177[a]	0.0708±0.0191	0.0485±0.0032	0.0264±0.0058
	0.4516±0.0903[b]	0.3512±0.0668	0.3749±0.0234	0.3222±0.0468
Lungs	0.1381±0.0133	0.1411±0.0187	0.0989±0.0073	0.0389±0.0041
	0.6730±0.0618	0.7093±0.0673	0.7646±0.0545	0.4787±0.0355
Liver	0.4107±0.0729	0.2596±0.0534	0.1915±0.0065	0.0536±0.0037
	2.0073±0.3907	1.2998±0.2151	1.4804±0.0402	0.6596±0.0182
Spleen	0.1168±0.0180	0.1043±0.0312	0.0736±0.0071	0.0396±0.0013
	0.5692±0.0883	0.7142±0.0938	0.5658±0.0513	0.4887±0.0288
Kidney	0.2526±0.0201	0.1857±0.0256	0.1433±0.0101	0.0584±0.0044
	1.2297±0.0794	0.9316±0.0734	1.1072±0.0730	0.7255±0.1003
Stomach	0.4660±0.0803	0.4367±0.0066	0.3827±0.0275	0.1612±0.0088
	2.2771±0.4241	2.2121±0.1748	2.9570±0.1933	2.0038±0.2537
Intestine	0.2415±0.0271	0.1812±0.0768	0.1617±0.0021	0.0687±0.0068
	1.1786±0.1407	0.9124±0.0651	1.2498±0.0074	0.8449±0.0492
Muscle	0.0652±0.0117	0.0585±0.0134	0.0330±0.0031	0.0250±0.0017
	0.3177±0.0555	0.2914±0.0436	0.2549±0.0232	0.2061±0.0287
Bone	0.1163±0.0087	0.0944±0.0109	0.0423±0.0027	0.0192±0.0051
	0.5668±0.0477	0.5026±0.0623	0.3270±0.0197	0.2383±0.0701
Thyroid	0.1894±0.0242	0.2722±0.0368	0.3004±0.0308	1.6524±0.0451
	0.9243±0.1285	1.3872±0.2575	2.3222±0.2392	20.4309±1.3928
Brain	***0.1125±0.0103***	***0.0363±0.0036***	***0.0147±0.0005***	***0.0112±0.0007***
	0.5488±0.0580	***0.1826±0.0054***	***0.1136±0.0042***	***0.1394±0.0180***
Carcass	0.6686±0.1160	0.6443±0.0370	0.3502±0.0226	0.1489±0.0041
	3.2482±0.9136	3.2768±0.4189	2.7079±0.1702	1.8469±0.1862

a. The values represent the mean ±SD for percent of injected dose per gram for 3 animals.
b. The values represent the mean ±SD for tissue-to-blood ratios for 3 animals.

Table 4.5. Biodistribution of ^{125}I-IAZA following i.v. administration in ligation groups with 2 hours recovery at various time intervals.

Tissue	Time (Hours) 2	4	8	24
Blood	0.2939±0.1199	0.2438±0.0346	0.1088±0.0070	0.1048±0.0064
Heart	0.2058±0.1079[a]	0.0985±0.0205	0.0529±0.0029	0.0419±0.0019
	0.6615±0.1334[b]	0.4050±0.0600	0.4885±0.0490	0.3538±0.0169
Lungs	0.2620±0.1192	0.1639±0.0206	0.0912±0.0192	0.0505±0.0030
	0.8699±0.0913	0.6714±0.0302	0.8431±0.1974	0.4047±0.0045
Liver	0.5482±0.0681	0.3922±0.1083	0.1932±0.0084	0.0841±0.0087
	1.8652±0.4478	1.6057±0.3450	1.7769±0.0414	0.6718±0.0361
Spleen	0.3038±0.1162	0.1313±0.0095	0.1299±0.0090	0.0621±0.0067
	1.0644±0.3434	0.5570±0.1304	1.1988±0.1288	0.4965±0.0326
Kidney	0.4300±0.2154	0.2229±0.0325	0.1888±0.0191	0.0946±0.0042
	1.4034±0.1622	0.9151±0.0470	1.7326±0.1020	0.7607±0.0619
Stomach	0.8916±0.2303	0.8168±0.1809	0.4307±0.0470	0.2941±0.0107
	3.2181±0.4518	3.3262±0.3859	3.9615±0.4217	2.3579±0.0572
Intestine	0.2417±0.0364	0.2330±0.0856	0.2203±0.0190	0.1102±0.0096
	0.9207±0.3306	0.9701±0.3319	2.0372±0.2585	0.8887±0.1217
Muscle	0.1959±0.1142	0.0583±0.0177	0.0534±0.0052	0.0338±0.0014
	0.6138±0.1557	0.2336±0.0435	0.4895±0.0161	0.2706±0.0040
Bone	0.2078±0.1261	0.1024±0.0156	0.0588±0.0107	0.0372±0.0042
	0.6440±0.1848	0.4210±0.0341	0.5440±0.1155	0.2972±0.0262
Thyroid	0.3294±0.0919	0.3849±0.1132	0.4188±0.0384	3.0766±0.0973
	1.1993±0.2582	1.5456±0.2733	3.8425±0.1500	27.8990±1.175
Brain	*0.1754±0.0784*	*0.0512±0.0065**	*0.0298±0.0059**	*0.0276±0.0021**
	0.5944±0.0674	*0.2104±0.0034**	*0.2703±0.0553**	*0.2656±0.0255**
Carcass	0.6288±0.1459	0.5842±0.0469	0.2352±0.0246	0.2178±0.0122
	2.3297±0.6650	2.4328±0.2995	2.1671±0.2517	1.7449±0.0589

a. The values represent the mean ±SD for percent of injected dose per gram for 3 animals.

b. The values represent the mean ±SD for tissue-to-blood ratios for 3 animals.

* Values significantly different from the control at $P < 0.05$ (t test).

At all 4 time intervals, the brain radioactivity in the ligation group, in terms of percentage of injected dose per gram, was higher than that of the control group. Statistic analysis showed that there were significant differences between the two groups at 4 hr, 8hr and 24 hr ($P<0.05$). These changes were probably due to the CBF and metabolism alteration during post-ischemia period in ligated gerbils. As it is shown in Figure 3.3, restoration of blood flow after ischemia leads to an initial short-lasting hyperemia in the brain.[97] Since the post-ischemia metabolic rate is initial low, the brain tissue must pass through a stage of transient hyperoxia during early recirculation period.[97] However, several studies have demonstrated that a secondary hypoperfusion developed within one hour after recirculation.[102-105] On the other hand, the metabolic rate of brain tissues gradually increases above the normal level over several hours of recirculation. This high metabolic need under low CBF state will give rise to a mismatch between oxygen demand and availability, resulting in a relative tissue hypoxia which leads to metabolic trapping of IAZA. Our radiolabeled compound was injected into gerbils after two hours of recirculation. At this time period, the CBF is below normal level and tissue hypoxia may exist in the brain of ligated gerbils. Therefore, ^{125}I-IAZA is presumed to be trapped in ischemic/hypoxic brain regions. This hypoperfusion state may reduce the delivery of ^{125}I-IAZA into the brain. However, between 4hr and 24hr, the brain radioactivity level in the ligation group was still higher than that of the control group. It is unlikely that this

higher uptake in ischemic/hypoxic brain is solely because reduced blood flow retards the clearance of bound and unbound compound. The CBF does not fall to zero under hypoperfusion state and gradually returns to the normal level after several hours of recircu-lation.[102-103] Therefore, the unbound compound was gradually cleared from the brain tissue while some compounds were selectively bound in the ischemia-induced hypoxic brain. This may explain why the higher brain radioactivity was seen in ligated gerbils at later time periods. On the other hand, the bilateral ligation only induces ischemia in forebrain and does not affect the circulation in cerebellum and hind brain. Our brain radioactivity data represent the total brain uptake. Therefore, it is possible that the different uptake between the two groups would be greater (>2:1) if we were to measure the radioactivity of focal ischemic/hypoxic regions.

The exact nature of the hypoxia-mediated metabolic reaction of IAZA remains undetermined. However, it is believed that IAZA, containing a 2-nitroimidazole base, would be preferentially activated through a series of enzyme mediated one-electron transfer reduction reactions in hypoxic tissues. This would result in selective binding of reactive reduction products of ^{125}I-IAZA with the cellular components. This selective binding character of the test compound has been well documented in both *in vitro* and *in vivo* studies.[5,8,9]

The relatively low radioactivity in brain tissues yielded lower brain-

to-blood ratios between 2hr and 24hr than other organ to blood ratios. At 2hr, the brain-to-blood ratios in the control and ligation groups reached the highest level of 0.5488 and 0.5944 respectively, but there is no significant difference between these two groups ($P>0.05$). Between 4hr and 24hr, the brain-to-blood ratios in ligated gerbils were significantly higher than those of control gerbils ($P<0.05$). However, these ratios were the lowest when compared to other organ-to-blood ratios. These data seemed to indicate that ^{125}I-IAZA might not be a suitable agent for brain imaging studies, as focal radioactivity needs to be greater than the background (e.g. brain to blood ratio >3:1) to record high-quality images. However, these ratios represent whole brain counts. It is possible that damaged areas of the brain might show significantly higher local concentrations of radioactivity.

The organ to blood ratios of radioactivity are shown graphically in Figures 4.4-4.7. Both groups showed high organ to blood ratios in stomach, intestine, liver and kidney at all 4 time intervals. Elevated levels of ^{125}I-IAZA activity in the stomach and intestine are often seen in biological distribution studies with radioiodinated pharmaceuticals and are believed to be an indication of free iodine. These organs are known to take up and accumulate iodine when it is released from iodinated compounds and occurs in circulation in the form of iodine anion. The relatively high hepatic radioactivity at 2hr is probably due to metabolism of ^{125}I-IAZA in the liver.[5] Although

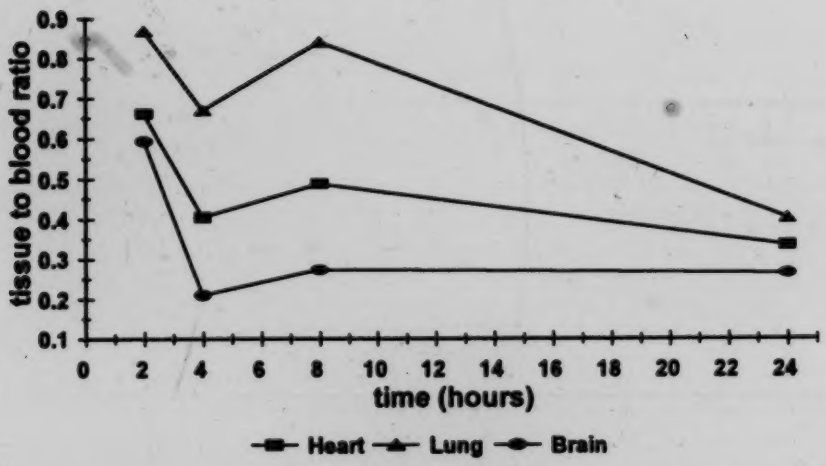

Figure 4.4. Tissue to blood ratios of radioactivity in heart, lung and brain at various time intervals following i.v. administration of ^{125}I-IAZA in ligated gerbils (n=3).

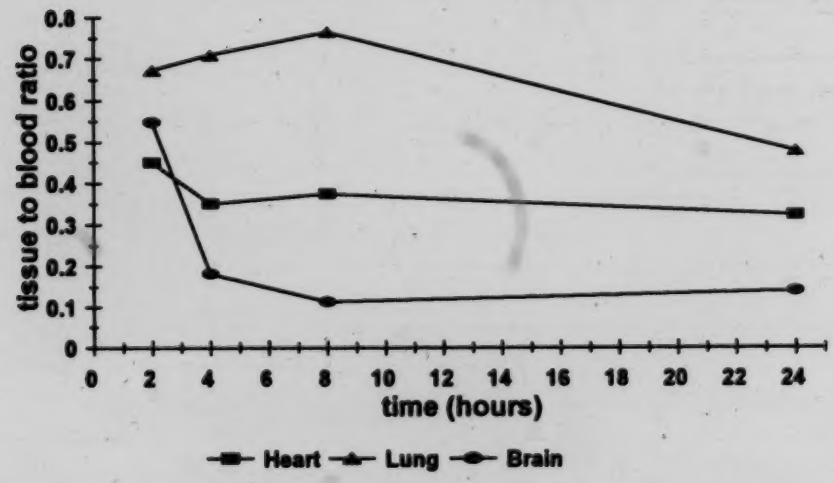

Figure 4.5. Tissue to blood ratios of radioactivity in heart, lung and brain at various time intervals following i.v. administration of ^{125}I-IAZA in control gerbils (n=3).

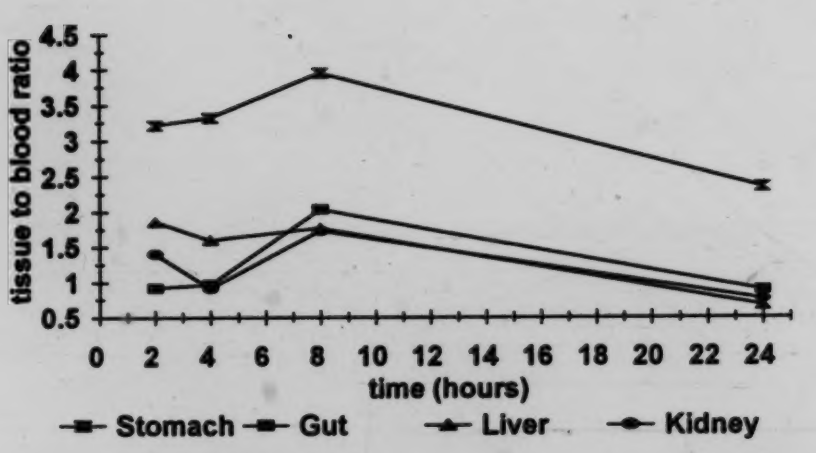

Figure 4.6. Tissue to blood ratios of radioactivity in stomach, gut, liver and kidney at various time intervals following i.v. administration of ^{125}I-IAZA in ligated gerbils (n=3).

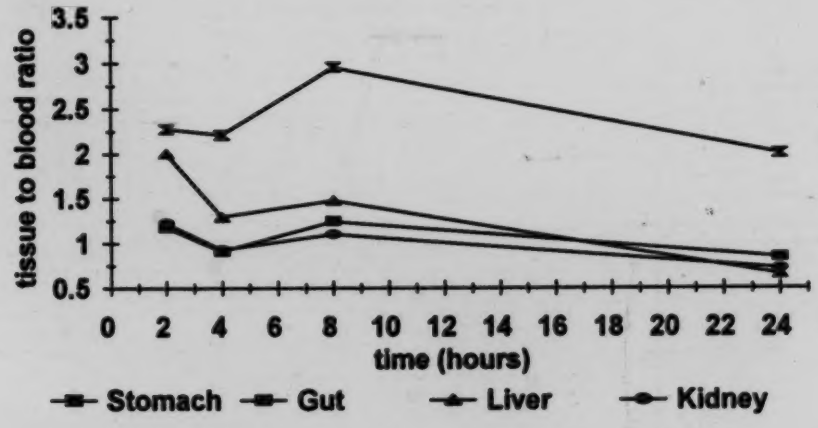

Figure 4.7. Tissue to blood ratios of radioactivity in stomach, gut, liver and kidney at various time intervals following i.v. administration of ^{125}I-IAZA in control gerbils (n=3).

the exact mechanism of the metabolism of ^{125}I-IAZA has not been determined, other biodistribution studies of IAZA in mice showed similar results.[5] This is not an unexpected result since nitroimidazoles have shown extensive oxidative metabolism in the liver and predominant excretion through the kidneys.[5] Therefore, it is reasonable to assume that similar oxidative reactions may occur with ^{125}I-IAZA, since it contains a 2-nitroimidazole base. Although no attempt was made to measure urinary radioactivity, the higher radioactivity in the kidneys, as well as the rapid whole-body elimination over the early time periods, suggests that the renal route of elimination is predominant. Biodistribution and scintigraphic studies in mice also support this mechanism of urinary excretion.[5]

The thyroid activity in the ligation and control groups reached a maximum of 16.55% and 10.75% respectively, of the total body radioactivity at 24hr. The increase in thyroid radioactivity (Table 4.6) is also a strong indication of *in vivo* metabolic deiodination of ^{125}I-IAZA, since thyroid is known to extract and accumulate circulating iodide anion. The release of I^- is a common phenomenon observed with a variety of iodinated compounds in animal and human studies.[5,11,10] This tendency has been addressed in human clinical studies with ^{123}I-IAZA where patients have their thyroid gland blocked against iodide uptake by the administration of Lugol's solution.[11,83]

Table 4.6. Thyroid radioactivity of ^{125}I-IAZA in the ligation and control groups.

	percent injected dose/organ		thyroid radioactivity as percentage of whole-body radioactivity	
Time	ligation	control	ligation	control
2 hr	0.11±0.05	0.07±0.02	0.62±0.38	0.45±0.12
4 h	0.11±0.02	0.10±0.01	0.69±0.15	0.66±0.07
8 hr	0.20±0.03	0.18±0.01	2.15±0.40	2.02±0.20
24 hr	1.20±0.14	0.70±0.06	16.55±3.10	10.75±2.30

The whole body elimination and blood clearance curves following i.v. administration of ^{125}I-IAZA into ligated and control gerbils are shown in Figures 4.8 and 4.9. The whole body activity at each time point was determined by adding up the radioactivity in all organs dissected plus the radioactivity in the remaining carcass. Whole blood radioactivity was calculated from an aliquot taken at the time of sacrifice, assuming blood to be 6.5% of the total body weight. The ^{125}I-IAZA activity remaining in the whole body at 2hr in the ligation and control groups represented 20.18% and 18.68% of injected dose respectively. This indicated a rapid initial elimination at early time period in both groups and provided additional support to the urinary excretion mode for elimination of this compound.

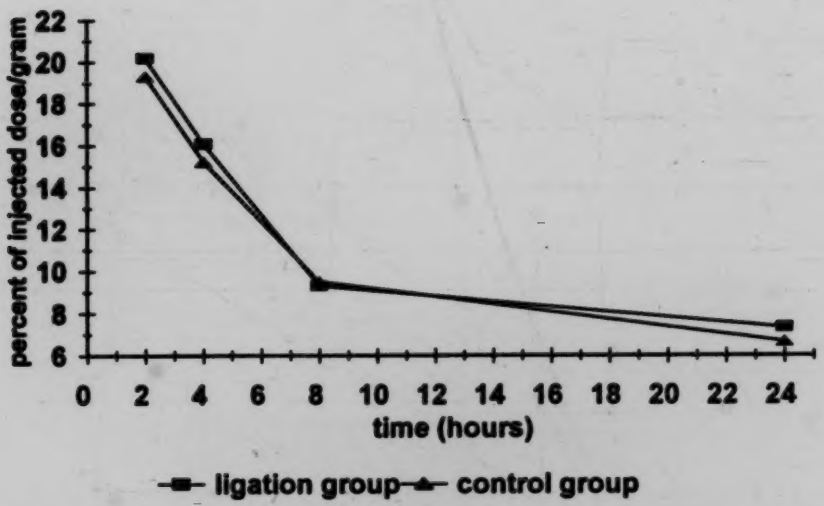

Figure 4.8. Whole-body elimination of radioactivity following i.v. administration of ^{125}I-IAZA in control (n=3) and ligation groups (n=3).

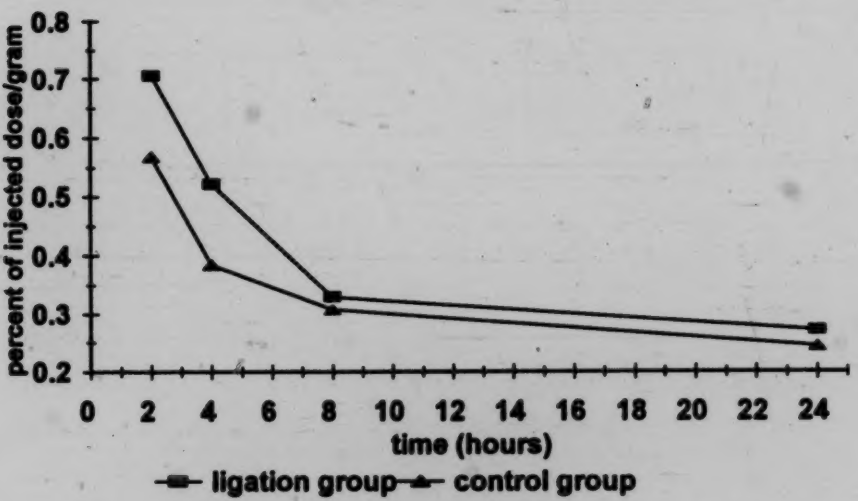

Figure 4.9: Blood clearance of radioactivity following i.v. administration of ^{125}I-IAZA in control (n=3) and ligation groups (n=3).

At longer periods, the elimination was much slower probably due to slow redistribution of the compound or its metabolic products from the tissues. Blood radioactivity clearance data in both groups showed similar behavior to whole body activity with an initial rapid decline in blood-radioactivity followed by a slower clearance at later time periods. Both whole-body elimination and blood clearance indicate a fast tissue clearance of radioactivity with little or no specific binding of the test compound to normal tissues or blood.

On the basis of the results discussed in this Section, it appears that there is no significant difference in ^{125}I-IAZA distribution between the ligation group and the control group. Both groups showed a rapid clearance of ^{125}I-IAZA from the body with more than 90% of the injected dose having been eliminated at 24 hr after injection. Even though the ligated gerbils showed higher activity in brain tissues than the control gerbils, the percent of injected dose per gram of brain and brain-to-blood ratios remained consistently lower than most other organs throughout the 24 hr period. These data suggested that IAZA might not be very suitable for imaging studies in our animal model.

4.5. Brain Section Study

Mongolian gerbils have two artery systems supplying the brain circulation: the carotid artery system supplies the cerebral hemisphere and the vertebral artery system supplies the cerebellum and hind brain.[86] Since most gerbils lack posterior communicating arteries (PCOA) between these two systems, bilateral carotid artery ligation can induce a high-grade bilateral cerebral ischemia, but will not affect the cerebellar circulation.[90,91] Many histological studies have demonstrated that bilateral carotid artery occlusion could cause typical ischemic neuronal damage in the forebrain regions, such as the hippocampus and the cerebral cortex.[88,96,97] However, similar damage is rarely seen in the cerebellum and brain stem.[97] Hoffman and Mathias both reported a greater uptake of ^{3}H and ^{18}F labeled MISO in the anterior regions of the right hemisphere in gerbils subjected to right carotid artery ligation.[6,83] However, their studies found no difference in posterior sections between left and right hemispheres. Our biodistribution studies showed a higher radioactivity in the brain of ligated gerbils. These results led us to undertake a brain sectioning study to determine the uptake of ^{125}I-IAZA in different brain regions in this gerbil stroke model.

The ligation group (n=7) was subjected to 5min of ligation; the control group (n=1) was sham-operated without ligation. All gerbils had two hours of recovery before they were injected with ^{125}I-IAZA. The neurological status of ligated gerbils was scored as stroke index

(see details in section 3.2.3.2). Based on the total score of stroke index, the ligated gerbils were classified as: group A-mildly symptomatic (SI≤5); group B-moderately symptomatic (SI =6-10); group C-severely symptomatic (SI>10). The specific activity of ^{125}I-IAZA was 13.1-39.3 GBq/mmol. Each animal received a dose of 803-977 KBq representing 8.8-21.7 μg of IAZA. Five hours after injection, the whole brain was removed and sliced coronally into 7 slices of approximately 1.5-2 mm thickness, designated A to G (Figure 4.10), from anterior to posterior sections. All slices were counted in a gamma scintillation counter. Statistic analysis was applied to test the significant differences in brain section uptake among these groups (see details in Appendix 2).

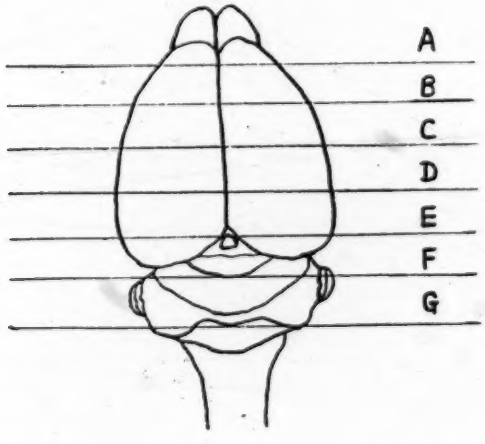

Figure 4.10. Dorsal view indicating brain sections through frontal planes.

Table 4.7 and Figure 4.11 & 4.12 showed the uptake of ^{125}I-IAZA in different brain regions in the control and ligation gerbils. There was fairly uniform uptake and no significant difference in all sections of the control animal. All control, sham-operated animals showed a stroke index of 0 and would not be expected to have any level of brain ischemia. In ligated gerbils, there was decreasing anterior to posterior binding of ^{125}I-IAZA in the brain, especially in groups B and C with stroke index greater than 10. The radioactivity in the anterior-middle sections (A-E), in terms of percent injected dose per gram and tissue to blood ratios, is up to twice that of posterior sections (F-G). The gerbil brain vasculature, along with the CBF and metabolism changes after ischemia, may explain this increase uptake in anterior-middle brain regions. Five minutes of bilateral ligation can induce complete ischemia in the forebrain areas of the ligated gerbils, but may not affect the blood circulation in the cerebellum and hind brain which is supplied by the vertebral system.[87-89] Therefore, these forebrain areas are the regions in which a secondary tissue hypoxia may develop due to an uncoupling between low CBF and high metabolism during the recirculation period. Since IAZA is known as a tracer of hypoxia in other systems, it is expected that this test compound could also be metabolically trapped in these ischemic/hypoxic forebrain areas which would result in a higher uptake in the anterior-middle brain sections. These results were in agreement with our distribution studies in gerbils. The overall higher uptake noted in the whole

brain can now be understood in terms of regional accumulation of ^{125}I-IAZA in areas expected to exhibit ischemia/hypoxia following bilateral ligation.

Table 4.7. Biodistribution of ^{125}I-IAZA in brain sections at 5hr following i.v. administration in the control and ligation groups.

	control(n=1)	ligation A (n=2)	ligation B (n=2)	ligation C (n=3)
stroke index	0[a]	5	10	12
section A	0.0152[b]	0.0200±0.0032	0.0265±0.0024	0.0341±0.0045
	0.0813[c]	0.1018±0.0161	0.1866±0.0131	0.2254±0.0328*
section B	0.0178	0.0222±0.0048	0.0348±0.0018	0.0457±0.0033*
	0.1035	0.1120±0.0112	0.2457±0.0178	0.3145±0.0204*
section C	0.0173	0.0234±0.0064	0.0376±0.0020	0.0454±0.0026*
	0.1006	0.1174±0.0159	0.2604±0.0032	0.3182±0.0069*
section D	0.0174	0.0224±0.0037	0.0331±0.0027	0.0398±0.0010*
	0.1012	0.1140±0.0073	0.2344±0.0109	0.2759±0.0062*
section E	0.0178	0.0213±0.0038	0.0267±0.0041	0.0368±0.0019*
	0.1035	0.1079±0.0051	0.1899±0.0179	0.2563±0.0121*
section F	0.0151	0.0195±0.0052	0.0193±0.0002	0.0208±0.0005
	0.0878	0.1030±0.0040	0.1290±0.0138	0.1306±0.0039
section G	0.0150	0.0185±0.0040	0.0183±0.0039	0.0205±0.0021
	0.0873	0.1022±0.0029	0.1148±0.0181	0.1202±0.0134

a. The number represents mean stroke index calculated at the time of injection (mean stroke index = sum of stroke index of the group/ number of animals in the group).
b. The number represents percent of injected dose per gram of brain tissue.
c. The number represents tissue-to-blood ratio.
* Values significantly different from the ligation group A at $P<0.01$(ANOVA).

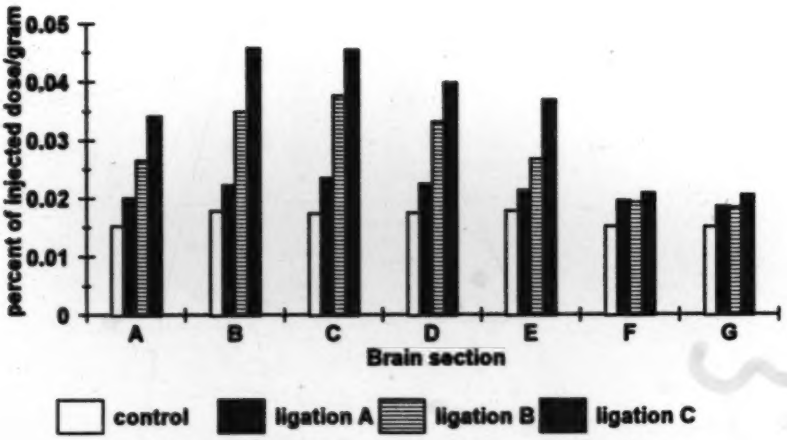

Figure 4.11. Percent of injected dose per gram of brain tissue at 5hr following i.v. administration of ^{125}I-IAZA in the control and ligation groups: group A (SI ≤ 5); group B (SI= 6-10); group C (SI >10).

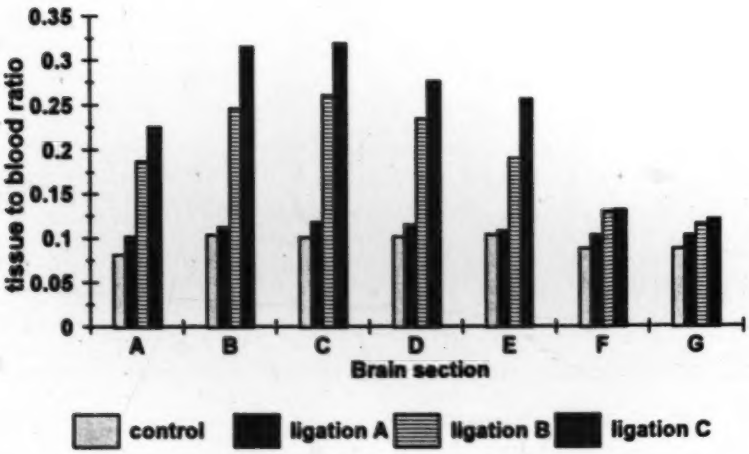

Figure 4.12. Tissue to blood ratios of radioactivity at 5hr following i.v. administration of ^{125}I-IAZA in the control and ligation groups: group A (SI ≤ 5); group B (SI= 6-10); group C (SI >10).

We also noted that the uptake of ^{125}I-IAZA in the anterior-middle sections in the ligation groups was higher than that of the control group, especially in the moderately (SI=6-10) and severely symptomatic (SI>10) groups. However, with only one control animal, it is mathematically impossible to use the statistic method to compare the control and the ligation groups. Since the ligation groups showed an increased brain section uptake as the stroke index increased, we used one-way ANOVA and Bonferroni multiple comparison procedures to see whether there are significant differences among these groups. The results showed that there were significant differences in uptake in the forebrain sections (A-E) among the three ligation groups ($P<0.05$). The uptake in the forebrain sections in the ligation group C is also significantly higher ($P<0.01$) than that of the ligation group A. However, there is no significant difference in uptake in the posterior brain sections (F-G) among the ligation groups ($P>0.05$). Though the percent injected dose per gram of tissue and brain-to-blood ratios were very low, the increased uptake in the forebrain sections seemed to be positively correlated with stroke index (Figure 4.13). Higher stroke index indicates more severe ischemic damage in the brain region, leading to increased uptake of the hypoxic binding agent ^{125}I- IAZA. These data were consistent with the findings from other laboratories.[6,83,134,135] Matsumoto et al reported a close relationship between brain pathologic lesions and stroke index.[135] Extensive ischemic neuronal damage was observed in symptomatic gerbils with high stroke index, but no lesion was detected in mildly symptomatic and sham-operated

control animals. Prior work by Ohon and Mastumoto has convincingly shown that there was a marked reduction in regional CBF in severely symptomatic gerbils and a lesser and variable reduction in animals with lower stroke index.[134,135] Therefore, ischemia and hypoxia are expected to be greater in these severely symptomatic gerbils leading to higher uptake of the hypoxia tracer ^{125}I-IAZA. Similar results were demonstrated in ^{18}F and ^{3}H labeled MISO studies in gerbils subjected to right carotid artery ligation.[6,83] Both studies showed statistically higher uptake of the test compounds in gerbils with a higher stroke index than in the control animals and those with a low stroke index.

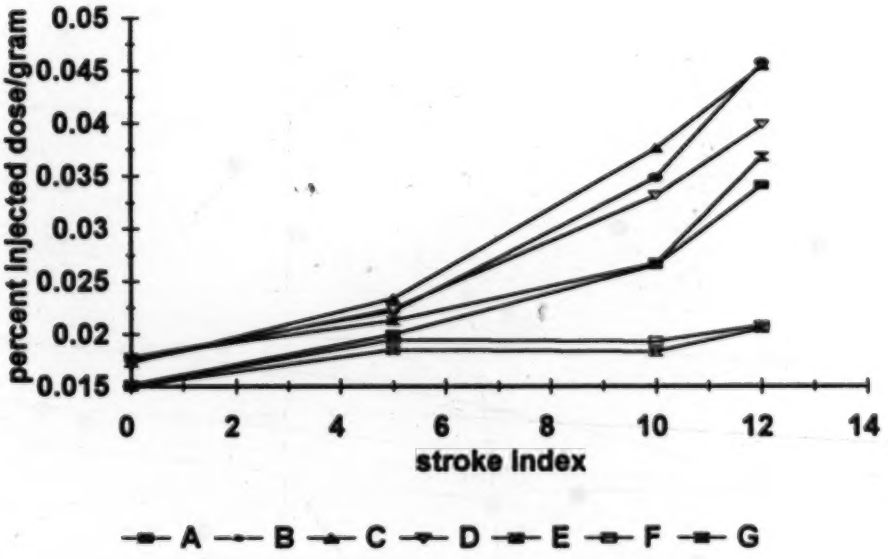

Figure 4.13. Percent of injected dose per gram of brain tissue in sections (A-G) plotted vs. stroke index in the control and ligation groups.

Our brain sectioning study indicated an increased uptake of ^{125}I-IAZA in the hypoxic/ischemic brain regions in ligated gerbils. This greater binding is also positively correlated with the severity of brain damage as indicated by stroke index. However, from this study, we could not conclude whether the radioactivity is evenly distributed in each slice or concentrated in certain structures that are more greatly damaged. An autoradiography study was performed to try and identify the areas of the brain that exhibit the most hypoxic damage following ligation.

4.6. Microscopic autoradiography

Several studies have suggested that IAZA, a misonidazole analogue, would undergo hypoxia-mediated metabolic reduction in hypoxic tumor tissue and become trapped in these tissues.[6-10] More recently, ^{125}I-IAZA binding in EMT-6 spheroids has shown that this binding is hypoxia-dependent and, in a manner similar to ^{3}H-MISO, can be detected by autoradiography.[10] In Matsumoto's work, the autoradiographic results demonstrated that an intense uptake of ^{3}H-MISO was diffuse and evenly distributed throughout the ischemic hemisphere ipsilateral to the ligation and was only sparsely distributed in the other side of the hemisphere.[135] From our biodistribution and brain sectioning studies, we also observed a higher uptake of ^{125}I-IAZA in the ischemic/hypoxic brain tissue of ligated gerbils than that of control gerbils. These results led us to employ autoradiography in

our study, since it may give an indication of which brain structure has a high uptake of the test compound.

The autoradiography study was performed in two animal groups (Table 4.8). In the first group, the ligated animals were subjected to 5 or 10 minutes of bilateral occlusion (two gerbils for each ligation protocol); whereas the control gerbil was subjected to the same surgical procedure without artery occlusion. In the second group, four gerbils were subjected to 5min of bilateral ligation and one gerbil was used as a control. All gerbils had two hours recovery before they were injected with ^{125}I-IAZA via the femoral vein. The specific activity of injected ^{125}I-IAZA was 13.1 or 39.3 GBq/mmol. Each animal received a dose of 1.84-5.08 MBq, representing 19.1-50.1 μg IAZA (Table 4.8). Five hours after injection, the animals were sacrificed by asphyxiation. The brain tissue was removed and fixed in 10% formalin, then dehydrated and embedded in wax. Serial 4μm brain sections were obtained and dipped in the liquid emulsion. After exposure in the emulsion for 6 weeks and followed by developing and fixing, sections were stained with H&E and observed under microscope(see detailed procedures in section 3.2.4.).

Silver grain density distribution was observed under a light microscope with oil immersion at a magnification of 100 using a grid of 100 squares (10um ×10um). Visible silver grains were counted over different anatomic brain sites as well as over background outside the

Table 4.8. General data of animals used in autoradiography studies.

Animal ID	ligation (min)	stroke index	^{125}I-IAZA specific activity (GBq/mmol)	^{125}I-IAZA injected (MBq)	brain weight (gram)	brain activity (KBq)
control#1	0	0	13.1	1.835	0.8021	44.1[a]
ligation#1	5	11	13.1	1.842	0.7845	64.9
ligation#2	5	12	13.1	1.854	0.8260	69.0
ligation#3	10	14	13.1	1.844	0.8607	71.4
ligation#4	10	14	13.1	1.847	0.8701	72.3
control#2	0	0	39.3	2.157	0.7866	51.0
ligation#5	5	12	39.3	5.076	0.7708	175.7
ligation#6	5	12	39.3	2.794	0.7842	98.6
ligation#7	5	11	39.3	2.226	0.7831	78.4
ligation#8	5	12	39.3	2.196	0.7895	78.0

a. The calculation of brain activity at 5hr after i.v. administration of ^{125}I-IAZA was based on our biodistribution data: estimated percent of injected dose/gram of brain tissue for the ligation and control gerbils at 5hr was 0.045 and 0.03, respectively. Brain activity = injected dose× brain weight × 0.045 (or 0.03)

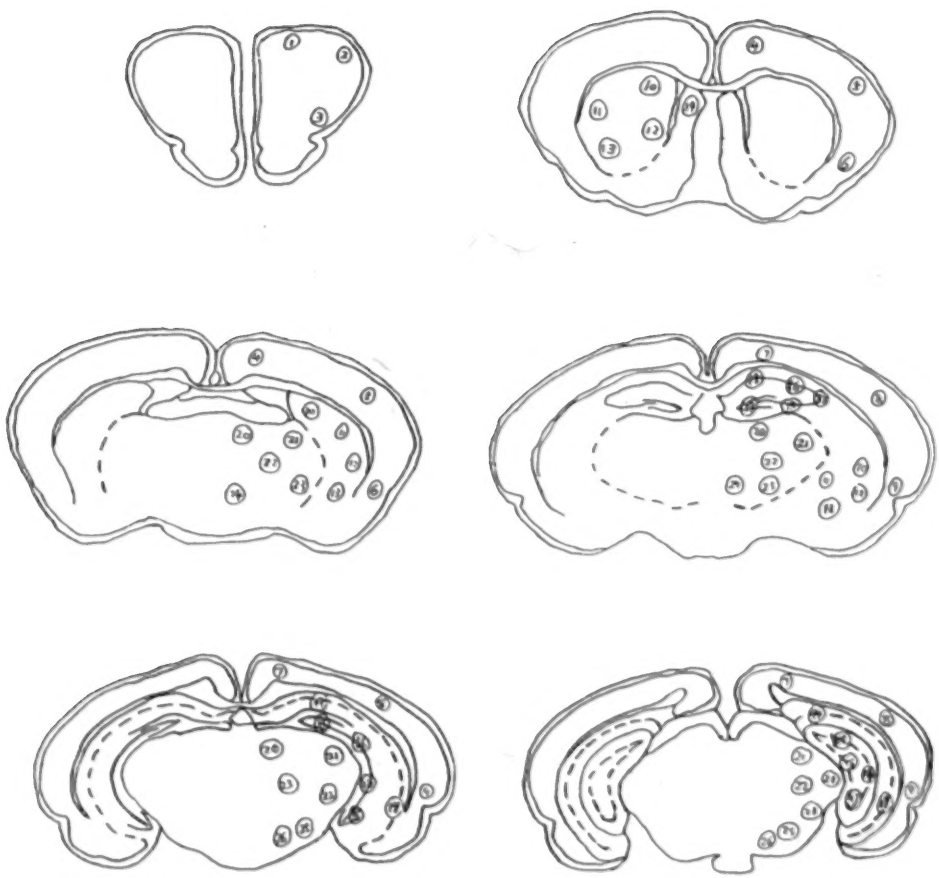

Figure 4.14: Anatomic sites of six coronal brain sections used for counting silver grains: front cortex (1-3), frontparietal cortex (4-6), parietal cortex (7-9), caudoputamen (10-13), septal nucleus (14), hippocampus (15-18), dentate gyrus (19), thalamus (20-23), hypothalamus (24) and substantia nigra (25-26).

tissue section on the slides. Figure 4.14 shows different anatomic sites used for counting silver grains, for example, the silver grains were counted in cortex, hippocampus, dentate gyrus, thalamus, hypothalamus, caudoputamen and septal nucleus in all gerbils. The frontal cortex and substantia nigra were not observed in the first group due to preparation and technical problems. The data was calculated as the number of silver grains per grid ($1mm^2$) with correction for background silver grains. The significant of differences in silver grain distribution over different anatomic sites were then compared between the control and ligation gerbils by using Student's t test (see Appendix 3).

Grain density over different anatomic regions in the control and ligated gerbils was listed in Table 4.8- 4.12. We noted that the amount of silver grains in all gerbils of the first group was lower than that of the second group. Since the auotradiographic studies were performed separately in these two groups, some factors such as total activity injected, processing method and dipping techniques may contribute to this difference. However, the results do indicated that the grain density in all ligated gerbils was always higher than that of control animals. In the first group (Table 4.9, 4.11 and Figure 4.14), the number of silver grains in all anatomic sites of ligated gerbils was significantly higher than that of the control one ($P<0.01$). The second group (Table 4.10,4.12 and Figure 4.15) also showed seminar higher grain density in the ligated gerbils ($P<0.01$).

Table 4.9. Mean silver grains per grid (1 mm^2) over autoradiographs in different anatomic sites in the control and ligated gerbils of the first group.

Brain section	control#1	ligation#1	ligation#2	ligation#3	ligation#4
Cortex					
frontparietal	28	64*	61*	78*	79*
parietal	25	56*	54*	69*	68*
Hippocampus	27	61*	62*	75*	78*
Dental gyrus	22	45*	44*	55*	56*
Thalamus	26	54*	55*	70*	68*
Hypothalamus	24	51*	50*	64*	61*
Caudoputamen	26	58*	56*	72*	70*
Septal nucleus	25	56*	53*	68*	67*

Table 4.10. Mean silver grains per grid (1 mm^2) over autoradiographs in different anatomic sites in the control and ligated gerbils of the second group.

Brain section	control#2	ligation#5	ligation#6	ligation#7	ligation #8
Cortex					
frontal	43	126*	105*	104*	110*
frontparietal	46	137*	119*	112*	121*
parietal	41	120*	99*	97*	102*
Hippocampus	48	145*	130*	122*	132*
Dental gyrus	36	103*	85*	82*	87*
Thalamus	40	116*	95*	94*	98*
Hypothalamus	38	106*	91*	90*	93*
Caudoputamen	46	133*	111*	110*	117*
Septal nucleus	44	127*	106*	105*	110*
Substantia nigra	34	97*	81*	80*	83*

* Values significantly different from the control at $P<0.01$ (t test).

Table 4.11. The ligation-to-control ratios of silver grains over different anatomic sites of the first group.

Brain section	control#1	ligation#1	ligation#2	ligation#3	ligation#4
Cortex					
frontparietal	1	2.29	2.18	2.79	2.82
parietal	1	2.24	2.16	2.76	2.74
Hippocampus	1	2.26	2.29	2.78	2.89
Dental gyrus	1	2.05	2.00	2.50	2.55
Thalamus	1	2.08	2.11	2.69	2.62
Hypothalamus	1	2.13	2.08	2.67	2.54
Caudoputamen	1	2.23	2.15	2.76	2.69
Septal nucleus	1	2.15	2.12	2.72	2.70

Table 4.12. The ligation-to-control ratios of silver grains over different anatomic sites of the second group.

Brain section	control#2	ligation#5	ligation#6	ligation#7	ligation #8
Cortex					
frontal	1	2.93	2.44	2.42	2.56
frontparietal	1	2.98	2.59	2.44	2.63
parietal	1	2.93	2.41	2.37	2.54
Hippocampus	1	3.02	2.70	2.54	2.75
Dental gyrus	1	2.86	2.36	2.28	2.42
Thalamus	1	2.89	2.37	2.35	2.45
Hypothalamus	1	2.79	2.37	2.37	2.44
Caudoputamen	1	2.89	2.41	2.40	2.54
Septal nucleus	1	2.89	2.41	2.39	2.50
Substantia nigra	1	2.85	2.38	2.35	2.44

*ratio = silver grains in the ligated gerbil/silver grains in the control gerbil).

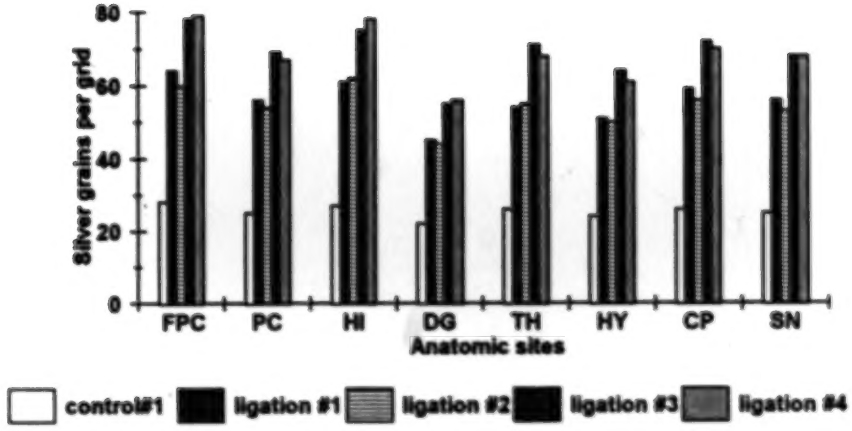

Figure 4.15. Mean silver grains per grid (1 mm^2) over autoradiographs in different anatomic sites in both control and ligated gerbils of the first group. (FPC-frontparietal cortex, PC-parietal cortex, HI-hippocampus, DG-dentate gyrus, TH-thalamus, HY-hypothalamus, CP-caudoputamen, SN-septal nucleus)

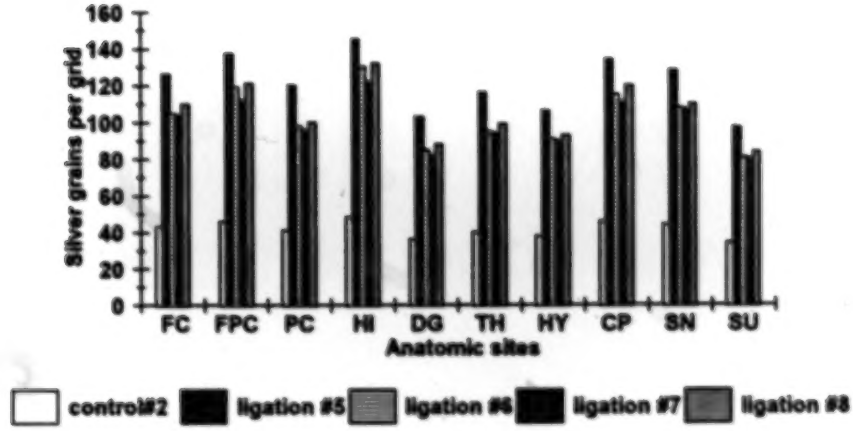

Figure 4.16. Mean silver grains per grid (1 mm^2) over autoradiographs in different anatomic sites in both control and ligated gerbils of the second group. (FC-front cortex, FPC-frontparietal cortex, PC-parietal cortex, HI-hippocampus, DG-dentate gyrus, TH-thalamus, HY-hypothalamus, CP-caudoputamen, SN-septal nucleus, SU-substantia nigra)

Compared to the control gerbils, the ligated gerbils had nearly three times more silver grains in all anatomic regions. These results demonstrated that ^{125}I-IAZA remained bound in the brain tissue through all procedures required to prepare autoradiographs. This increase silver grain density was in agreement with our previous biodistribution and brain sectioning studies which showed higher radioactivity in brain tissues of ligated gerbils.

In addition, in two gerbils subjected to 10 min ligation, there were significantly higher amount of silver grains when compared with those of the two gerbils subjected to 5min ligation ($P<0.05$). Longer ischemia insult could cause more severe ischemic/hypoxic damage in the brain tissue as indicated by higher stroke index which leads to more uptake of ^{125}I-IAZA in these damaged regions. This finding is consistent with our brain sectioning study which showed a positive correlation between the stroke index and the accumulation of ^{125}I-IAZA in forebrain brain regions.

Comparing the number and the ratio of silver grains among different anatomic sites (Table 4.9-4.12), the cerebral cortex and hippo-campus areas seemed to have the highest level. This is presumably because these two brain structures are known to be very vulnerable to ischemic insult.[109,138] Studies in animals have shown that regional blood flow is more severely reduced in the cerebral cortex and

hippocampus than in other brain regions during and after experienced stroke.[103,134,] Histological literature has also demonstrated that neuropathological damage is most frequently seen in these two areas.[109,138]

All the above results seemed to indicate that ^{125}I-IAZA was bound to hypoxic/ischemic brain tissue in ligated gerbils. However, we also found that the number of silver grains per grid is relative low. This is probably due to the low brain radioactivity and processing techniques. By the time of sacrifice, the estimated radioactivity in the whole brain was lower than 100 KBq in all animals except one ligated one (Table 4.8). Also, only the anterior-middle part of the brain was used for further processing which meant less radioactivity remained in the brain. The brain tissues also went through a series of dehydrating and fixing procedures. This could have washed out unbound compound and may have removed some bound compound as well. The above preparation procedures usually required two weeks and the slices were exposed in the emulsion for six weeks. Therefore, decay would have reduced the overall activity in these samples during the contact period. In summary, all these factors affected the amount of radioactivity that remained in brain tissues and resulted in the relative low number of silver grains in our study.

CONCLUSION

The primary objective of the study described in this thesis was to evaluate the potential of radioiodinated iodoazomycin arabinoside (IAZA) as a non-invasive tracer of brain ischemia/hypoxia following stroke. The *in vivo* studies reported in the previous chapters have now led to the following conclusions.

1. IAZA can be radioiodinated by exchange labeling using pivalic acid melt method with high radiochemical yield (>80%). The reaction product can be purified by using silica gel column chromatography with a radiochemical purity greater than 95%.

2. The bilateral common artery occlusion method successfully induces forebrain brain ischemia in Mongolian gerbils. Longer ligation periods can cause more severe brain damage as indicated by neurological signs and stroke index.

3. In *in vivo* biodistribution studies with ^{125}I-IAZA in both ligated and control gerbils, this tracer showed a relatively lower percent of injected dose per gram of the brain tissue (absolute uptake) and lower brain-to-blood ratios (specific uptake) up to 24hr than in most other organs. Although the ligation groups had higher uptake of ^{125}I-IAZA in the brain tissue than that of control groups, these data

indicated that the test compound might not be an ideal agent for imaging study. The higher uptake in other organs would also complicate the use of this compound due to dosimetry issues. *In vivo* deiodination was followed by subsequent accumulation of radioactivity in the thyroid gland. ^{125}I-IAZA was rapidly eliminated from the body with more than 90% of the injected dose having been eliminated within 24hr after injection in both groups.

4. Brain section studies showed higher uptake of ^{125}I-IAZA in the anterior-middle brain regions of ligated gerbils relative to sham operated controls. This increased uptake was positively correlated with the severity of brain damage as indicated by stroke index.

5. Microscopic autoradiography demonstrated the ^{125}I-IAZA distribution over different anatomic brain sites. An increase in silver grain density was noted in all anatomic sites of ligated gerbils. This finding was in agreement with our previous biodistribution and brain sectioning studies.

6. This study has some limitations. First of all, only one basic protocol for time (five hours after injection) was used to localize our compound and a better protocol may exist. Secondly, this gerbil stroke model is not a true indication of human situation. Therefore, the relevance of some experimental data to the human condition remains to be determined.

Based on our studies, there is a significantly higher uptake of ^{125}I-IAZA in the brain tissue of ligated gerbils than that of control ones. Though the percent of injected dose per gram of brain and the brain-to-blood ratios are relatively lower than most other organ, the increase uptake may indicate that this compound is selectively bound to ischemic/ hypoxic brain tissue in ligated gerbils. From this limited study, it is not possible to speculate the potential role of this compound in clinical investigations and treatment of the stroke. Further study may reveal the potential of radiolabeled IAZA as a imaging agent to evaluate brain hypoxia following stroke.

REFERENCES:

1. Wolf PA, Cobb JL, D'Agostino RB: Epidemiology of stroke. In Barnett HJM., Mohr JP, Stein BM, Yatsu FM (eds): Stroke: pathophysiology, diagnosis and management. p.3, Churchill Livingstone, New York, 1992

2. Astup J, Siesjo BK, Symon L: Thresholds in cerebral ischemia — the ischemic penumbra. Stroke 12: 723, 1981

3. Heiss WD, Fink GR, Hubber M, Herholz K: Positron emisssion tomography imaging and the therapeutic window. Stroke 24 (suppl) : 50, 1993

4. Fisher M, Sotak CH, Minematsu K, Li L: New magnetic resonance techniques for evaluating cerebrovascular disease. Annal. Neurol. 32: 115, 1992

5. Mannan RH: Novel non-invasive markers of tumor hypoxia. Ph.D Thesis, Department of Pharmacy and Pharmaceutical Sciences, University of Alberta, Edmonton, Canada, 1991

6. Mathias CJ, Welch MJ, Kilbourn MR, Jerabek PA, Patrick TB, Raichle ME, Krohn KA, Rasey JS, Shaw DW: Radiolabelled hypoxic cell: tracers for assessment of ischemia. Life Sci. 44: 199, 1989

7. Yeh SH, Liu RS, Hu HH, Chang CP, Chu LS, Chou KL, Wu LC: Ischemic penumbra in acute stroke: demonstrating by PET with fluorine 18 fluoromisonidazole. J. Nuc. Med. 35: 142p, 1994

8. Mannan RH, Somayaji VV, Lee J, Mercer JR, Chapman JD, Wiebe LI: Radioiodinated 1-(5-iodo-5-deoxy-β-D-arabinofuranosyl)-2-nitroimidazole (iodoazomycin arabinoside: IAZA): a novel marker of tissue hypoxia. J. Nuc. Med. 32: 1764, 1991

9. Mercer JR, Mannan RH, Somayaji VV, Lee J, Chapman JD, Wiebe LI: Sugar-coupled 2-nitroimidazoles: novel *in vivo* markers for hypoxic tumor tissue. In Maddelena DJ, Snowdon GM, Boniface GR: Advances in Radiopharmacology. Proceedings of the Sixth International Symposium on Radiopharmacology. p.104, Wollongong University Press, Wollongong, Australia, 1990

10. Parliament MB, Chapman JD, Urtasun RC, McEwan AJ, Golberg LE, Mercer JR, Mannan RH, Wiebe LI: Non-invasive assessment of human tumor hypoxia with ^{125}I-iodoazomycin arabinoside: preliminary report of a clinical study. Brit. J. Cancer. 65: 90, 1992

11. Groshar D, McEwan AJ, Parliament MB, Urtasun RC, Golberg LE, Hoskinson M, Mercer JR, Mannan RH, Wiebe LI, Chapman JD: Imaging tumor hypoxia and tumor perfusion. J. Nuc. Med. 34: 885, 1993

12. Hossmann KA: Viability thresholds and the penumbra of focal ischemia. Ann. Neurol. 36: 557, 1994

13. Heiss WD, Graf R: The ischemic penumbra. Curr. Opin. Neurol. 7: 11, 1994

14. Mohr JP: Overview of laboratory studies in stroke. In Barnett HJM, Mohr JP, Stein BM, Yatsu FM (eds): Stroke: pathophysiology, diagnosis and management. p.149, Churchill Livingstone, New York, 1992

15. Kaps M, Damian MS, Teschendorf U, Dorndorf W: Transcranial Doppler ultrasound findings in middle cerebral artery occlusion. Stroke. 21: 532, 1990

16. Frankowiak RSJ, Wise RJS: Positron emission in ischemic cerebrovascular disease. Neurol. Clin. North. Am. 1: 183, 1983

17. Barnett HJM: Management of cerebral vascular problems: neurological and neurosurgical view points. In Barnett HJM, Mohr JP, Stein BM, Yatsu FM (eds): Stroke: Pathophysiology, diagnosis and management. p.921, Churchill Livingstone, New York, 1986

18. Grotta JC: Antithrombotic therapy in acute cerebral ischemia. In Barnett HJM, Mohr JP, Stein BM, Yatsu FM (eds): Stroke: pathophysiology, diagnosis and management. p.943, Churchill Livingstone, New York, 1992

19. Siesjo BK: Pathophysiology and treatment of focal cerebral ischemia. Part II: Mechanisms of damage and treatment. J. Neurosurg. 7: 337, 1992

20. Hakim AM, Evans AC, Berger L, Kuwabara H, Marchal G, Worsley K, Biel C, Pokrupa R, Diksic M, Meyer E, Gjedde A, Marrett S: The effect of nimodipine on evolution of human cerebral infarction studied by PET. J. Cere. Blood Flow Metab. 9: 523, 1989

21. Ambrose J: Computerized transverse axial scannin (tomography): 2. clinical application. Br. J. Radiol. 46: 1023, 1973

22. Bradac GB, Oberson R: Angiography and computed tomography in cerebro-arterial occlusion disease. Springer-Verlag, New York, 1983

23. Heiss WD, Herholz K, Bocher-Schwarz HG, Pawlik G, Wienhard K, Steinbrich W, Friedmann G: PET, CT and MR imaging in cerebrovascular disease. J. Comput. Assist. Tomogr. 10: 903, 1986

24. Hilal SK, Mohr JP: Magnetic resonance scanning. In Barnett HJM, Mohr JP, Stein BM, Yatsu FM (eds): Stroke: pathophysiology, diagnosis and management. p.189, Churchill Livingstone, New York, 1992

25. Mussel F, Wegmuller H, Huber P: Comparison of magnetic angiography, magnetic resonance imaging and conventional angiography in cerebral arteriovenous malformation. Neuroradiology 33 : 56, 1991

26. Kertesz A, Black SE, Nicholson L, Carr T: The sensitivity and specificity of magnetic resonance imaging in stroke. Neurology 37: 1580, 1987

27. Savoiardo M, Bracchi M, Passerini A, Visciani A: The vascular territories in cerebellum and brainstem: CT and MR study. Am. J. Neuroradiology. 8: 199, 1987

28. Masdeu JC, Brass LM: SPECT imaging of stroke. J. Neuroimag. 5: s14, 1995

29. Bose A, Pacia SV, Fayad P: Cerebral blood flow (CBF) imaging compared to CT during the initial 24 hours of cerebral infarction. Neurology 40 (suppl.1): 190, 1990

30. Seiderer M, Krappel W, Moser E, Hahn D, Schmiedek P, Buell U, Kirsch CM, Lissner J: Detection and quantification of chronic cerebrovascular disease: comparison of MR imaging, SPECT and CT. Radiology 170: 545, 1989

31. Alexandrov AV, Bladin CF, Ehrlich LE, Black SE: Clinical significance of increased uptake of HMPAO on brain SPECT scans in acute stroke. J. Neuroimag. 6: 150, 1996

32. Moretti JL, Defer G, Cinotti L, Cesaro P, Degos JD, Vigneron N, Ducassou D, Holman BL: "Luxury perfusion" with ^{99m}Tc-HMPAO and ^{123}I-IMP SPECT imaging during the subacute phase of stroke. J. Nucl. Med. 16: 17, 1990

33. Raynaud C, Rancurel G, Tzourio N, Soucy JP, Baron JC, Pappata S, Cambon H, Mazoyer B, Lassen NA, Cabanis E: SPECT analysis of recent cerebral infarct. Stroke 20: 192, 1989

34. Mountz JM, Deutsch G, Khan SH: Regional cerebral blood flow changes in stroke imaged by Tc-99m HMPAO SPECT with corresponding anatomic image comparison. Clin. Nucl. Med. 18: 1067, 1993

35. Baron JC: Positron emission tomography studies in ischemic stroke. In: Barnett HJM, Mohr JP, Stein BM, Yatsu FM (eds): Stroke: pathophysiology, diagnosis and management. p.111, Churchill Livingstone, New York, 1992

36. Baron JC, Rougemont D, Bousser MG, Lebrun-Grandie P, Iba-Zizen MT, Chiras J: Local CBF, oxygen extraction fraction (OEF) and $CMRO_2$: prognostic value in recent supratentorial infarction in humans. J. Cere. Blood Flow Metab. 3 (suppl A): S1, 1983

37. Hakim AM: Hemodynamic and metabolic studies in stroke. Semin. Neurol. 9: 286, 1989

38. Powers WJ: Cerebral hemodynamics in ischemic cerebrovascular disease. Am. Neurol. 29: 231, 1991

39. Hakim AM, Hogan MJ: In vivo binding of nimodipine in the brain: the effect of focal cerebral ischemia. J. Cere. Blood Flow Metab. 11: 762, 1991

40. Fisher M: Potentially effective therapies for acute ischemic stroke. Europ. Neurol. 34: 3, 1995

41. Baron JC: Pathophysiology of acute cerebral ischemic: PET studies in human. Cerebrovascular Disease. 1(suppl): 22, 1991

42. Rieth W, Hasegawa Y, Latour LL: Multi-slice diffusion mapping for 3-D evolution of cerebral ischemia in a rat stroke model. Neurology 45: 172, 1995

43. Hasegawa Y, Fisher M, Latour LL: MRI diffusion mapping of reversible and irreversible ischemic injury in focal ischemia. Neurology 44: 1484, 1994

44. Di Rocco RJ, Kuczynski BL, Pirro JP, Bauer A, Linder KE, Ramalingam K, Cyr JE, Chan YW, Raju N, Narra RK, Nowotnik DP, Nunn AD: Imaging ischemic tissue at risk of infarction during stroke. J. Cereb. Blood Flow Metab. 13: 755, 1993

45. Webster LT: Drugs used in chemotherapy of protozal infections. In Gliman AG, Rall TW, Nies AS, Taylor P(eds): The pharmacological basis of therapeutics. p.1002, Pergamon, New York, 1990

46. Edwards DI: Nitroimidazole drugs-action and resistance mechanism. J. Antimicrob. Chemother. 31: 9, 1990

47. Denekamp J, Harris SR: Tests of two electron affinic radiosensitizers *in vivo* using regrowth of experimental carcinoma. Radiat. Res. 61: 191, 1975

48. Hall EJ, Roizen-Towle L: Hypoxic sensitizers: radiobiological studies at the cellular level. Radiology 117: 453, 1975

49. Petersen EO: Radiosensitizing and toxic effects of the 2-nitroimidazole Ro-07-0582 in different phases of the cell cycle of extremely hypoxic cells *in vitro*. Radiat. Res. 73: 180, 1978

50. Fowler JF, Denekamp J: A review of hypoxic cell radiosensitization in experimental tumors. Pharmacol. Ther. 7: 413, 1979

51. Franko AJ, Chapman JD, Koch CJ: Binding of misoimidazole to EMT-6 and V79 spheroids. Int. J. Radiat. Oncol. Biol. Phys. 8: 737, 1982

52. Raleigh JA, Franko AJ, Koch CJ, Born JL: Binding of misonidazole to hypoxic cells in monolayer and spheroid culture : Evidence that side-chain label is bound as effectively as a ring label. Br. J. Cancer. 51: 229, 1985

53. Miller GG, Ngan-Lee J, Chapman JD: Intracellular localization of radioactively-labeled misonidazole in EMT-6 tumor cells in vitro. Int. J. Radiat. Oncol. Biol. Phys. 8: 741, 1982

54. Garrecht BM, Chapman JD: The labeling of EMT-6 tumors in Balb/c mice with ^{14}C -misonidazole. Bri. J. Radiol. 56: 745, 1983

55. Urtasum RC, Koch CJ, Franko AJ, Raleigh JA, Chapman JD: A novel technique for measure human tissue PO_2 at the cellular level. Bri. J. Cancer. 54: 453, 1986

56. Urtasum RC, chapman JD, Raleigh JA, Franko AJ, Koch CJ: Binding of ^{3}H-misonidazole to solid human tumors as a measure of tumor hypoxia. Int. J. Radiat. Oncol. Biol. Phys. 12: 1263, 1986

57. Rasey JS, Hoffman JM, Spence AM, Krohn KA: Bromomisonidazole: synthesis and characterization of a new radiosensitizer. Radiat. Res. 91: 542, 1982

58. Jette DC, Wiebe LI, Chapman JD: Synthesis and *in vivo* studies of the radiosensitizer 4-[^{82}Br]-bromomisonidazole. Int. J. Nucl. Med. Biol. 10: 205, 1983

59. Rasey JS, Wui-Jim K, Grierson JR, Graunbaum Z, Krohn KA: Radiolabelled fluoromisonidazole as an imaging agent for tumor hypoxia. Int. J. Radiat. Oncol. Biol. Phys. 17: 985, 1989

60. Wasserman TH, Stetz J, Phillips TL: Clinical trials of misonidazole in the United States. Cancer. Clini. Trials. 4: 7, 1981

61. Overgaard J, Horsman MR: Modification of hypoxia-induced radioresistance in tumors by the use of oxygen and sensitizer. Semi. in Radiat. Oncol. 6(1):10, 1996

62. Paliament MB, Wiebe LI, Franko AJ: Nitroimidazole adducts as markers for tissue hypoxia:mechanistic studies in aerobic noraml tissues and tumor cell. Br. J. Cancer 66:1103, 1992

63. Edwards DI: Reduction of nitroimidazoles in vitro and DNA damage. Bochem. Pharmacol. 35: 53, 1986

64. Gowrisankar ICR, Phadke RP, Oza SD, Talwalker S: Experimental evaluation of activity against anaerobic bacteria in vitro and in animal models of anaerobic infection. J. Antimicrob. Chemother. 15: 463, 1985

65. Rauth AM, McClelland RA, Michaels HB, Batistella R: The oxygen dependence of the reduction of nitroimidazole in a radiolytic model system. Int. J. Radiat. Oncol. Biol. Phys. 10: 1323, 1984

66. Chapman JD, Baer K, Lee J: Characteristics of the metabolism induced binding of misonidazole to hypoxic mammalian cells. Cancer. Res. 43: 1523, 1983

67. Smith BR, Born JL: Metabolism and excretion of [^{3}H]-misonidazole by hypoxic rat liver. Int. J. Radiat. Oncol. Biol. Phys. 10: 1365, 1984

68. Varghese AJ, Gulyas S, Mohindra JK: Hypoxia-dependent reduction of 1-(2-nitro-1-imidazolyl)-3-methoxy-2-propanol by chinese hamster ovary cells and KHT tumor cells *in vitro* and *in vivo*. Cancer. Res. 36: 3761, 1976

69. Koch RL, Rose C, Rich TA, Goldman P: Comparative misonidazole metabolism in anaerobic bacteria and hypoxic chinese hamster lung fibroblast (V-79-473) cells. Biochem. Pharmacol. 31: 411, 1982

70. Franko AJ: Misonidazole and other hypoxic markers: metabolism and applications. Int. J. Radiat. Oncol. Biol. Phys. 12: 1195, 1986

71. Mason PR, Holztman JL: The role of catalytic super oxide formation in the O_2 inhibition of nitroreductase. Biochem. Biophys. Res. Comm. 67:1267, 1975

72. Perez RE, Kalyanaraman B, Manson RP: The reduction metabolism of metronidazole and ronidazole by aerobic liver microsomes. Mol. Pharmacol. 17: 17,1980

73. Whitmore GF, Varghese AJ: The biological properties of reduced nitroheterocylics and possible underlying biochemical mechanism. Biochem. Pharmacol. 35: 97, 1986

74. Varghese AJ, Whitmore GF: Binding of nitroreduction products of misonidazole to nucleic acids and proteins. Cancer. Clin. Trials. 3: 43, 1980

75. Weissburger JH, Weissburger EK: Biochemical formation and pharmacological toxicological and pathological properties of hydroxylamines and hydroxamic acids. Pharmacol. Rev. 25: 1, 1973

76. LaRusso NF, Tomasz M, Muller M, Lipman R: Interaction of metronidazole with nucleic acids in vitro. Mol. Pharmacol. 13: 872, 1977

77. Raleigh JA, Koch CJ: Importance of thiols in the reductive binding of 2-nitroimidazoles to macromolecules. Biochem. Pharmacol. 40: 2457, 1990

78. Cline JM, Thrall DE, Page RL, Franko AJ, Raleigh JA : Immunohistochemical detection of hypoxia marker in spontaneous canine tumours. Br. J. Cancer. 62: 925, 1990

79. Jette DC, Wiebe LI, Flanagan RJ, Lee J, Chapman JD: Iodoazomycin riboside (1-[5-iodo-5-deoxy-ribofuranosyl]-2-nitroimidazole), a hypoxic cell marker: I. Synthesis and *in vitro* characterization. Radiat. Res. 105: 169, 1986

80. Wiebe LI, Jette DC, Chapman JD, Flanagan RJ, Meeker BE : Iodoazomycin riboside (1-[5-iodo-5-deoxy-ridofuranosyl]-2-nitroimidazole), a hypoxic cell marker. *In vivo* evaluation in experimental tumors. Nucl. Med. Clin. Oncol. 21: 402, 1986

81. Al-Arafaj A, Ryan EA, Hutchison K, Mannan RH, Mercer J, Wiebe LI, McEwan AJ: An evaluation of ^{123}I-iodoazomycin arabinoside (IAZA) as a marker for tissue hypoxia in patients with diabetes mellitus. Eur. J. Nuc.Med. 21:1338, 1994

82. Rasey JS, Hoffman JM, Spence AM, Krohn KA: Hypoxic mediated binding of misonidazole in non-malignant tissue. J. Radiat. Oncol. Biol. Phys. 12: 1255, 1986

83. Hoffman JM, Rasey JS, Spence AM, Shaw DW, Krohn KA: Binding of the hypoxia tracer [^{3}H] MISO in cerebral ischemia. Stroke 18: 168, 1987

84. Kahn K: The natural cause of experimental cerebral infarction in the gerbil. Neurology 22: 510, 1972

85. Levine S, Payan H: Effects of ischemia and other procedures on the brain and retina of the gerbil. Exp. Neurol. 16: 255, 1966

86. Levine S, Sohn D: Cerebral ischemia in infant and adult gerbils. Arch. Pathol. 87: 315, 1969

87. Levy DE, Brierley JB: Communications between vertebral-basilar and carotid arterial circulation in the gerbil. Exp. Neurol. 45: 503, 1974

88. Berry K, Wisniewski HM, Svarzbein L, Baez S: On the relationship of brain vasculature to production of neurological deficit and morphological changes following unilateral common carotid artery ligation in gerbils. J. Neurol. Sci. 25: 75, 1975

89. Harrison MJ, Brownbill D, Lewis PD, Russell RW: Cerebral edema following carotid artery ligation in the gerbil. Arch. Neurol. 28: 389, 1973

90. Mayevsky A, Breuer Z: The Mongolian gerbil as a model for cerebral ischemia. In Schurr A, Rigor BM (eds): Cerebral ischemia and resuscitation. p. 29, CRC Press, Boca Raton, Florida, 1990

91. Breuer Z: Determination of brain vasculature in the Mongolian gerbil and the biochemical correlated responses under ischemia. M.Sc. Thesis, Department of Life Sciences, Bar Ilan University, Israel, 1988

92. Mayevsky A, Zarchin N, Tannebaum B: Brain responses to experimental oxygen deficiency in the Mongolian gerbil. In Bruley D, Bicher HI, Reneau D (eds): Oxygen transport to tissue (VI). p.191, Plenum Press, New York, 1984

93. Mayevsky A, Friedli CM, Reivich M: Metabolic, ionic and electrical responses of the gerbil brain to ischemia. Am. J. Physiol. 248: R99, 1985

94. Crockard A, Iannotti F, Hunstock AT, Harris RJ, Symon L: Cerebral blood flow and edema following carotid occlusion in the gerbil. Stroke 11: 494, 1980

95. Osburne RC, Halsey JH: Cerebral blood flow. A predictor of recovery from ischemia in the gerbil. Arch. Neurol. 32: 457, 1975

96. Kirino T, Sano K: Selective Vulnerability in the gerbil hippocampus following transient ischemia. Acta. Neurol. 62: 201, 1984

97. Siesjo BK: cell damage in the brain: a speculative synthesis. J. Cere. Blood Flow Metab. 1: 155, 1981

98. Mabe H, Lomqvist P, Siesjo BK: Intracellular PH in the brain following transient ischemia. J. Cereb. Blood Flow Metab. 3: 109, 1983

99. Yanagihara T, McCall JT: Ionic shift in cerebral ischemia. Life Sci. 30: 1921, 1982

100. Kuschinsky W, Wahl M, Bosse O, Thurau K: Perivascular potassium and PH as determinants of local pial arterial diameter in cats. A microapplication study. Circ. Res. 31: 240, 1972

101. Dienel GA, Pulsinelli WA, Duffy TE: Regional protein synthesis in the rat brain following acute hemispheric ischemia. J. Neurochem. 35 : 1216, 1980

102. Levy DE, Uitert RLV, Pike CL: Delay postischemic hypoperfusion: a potentially damaging consequence of stroke. Neurology 29: 1245, 1979

103. Suzuki R, Yamaguchi T, Li CL, Klatzo I: The effects of 5 minutes ischemia in Mongolian gerbils: I Blood-brain barrier, cerebral blood flow and local cerebral glucose utilization changes. Acta. Neuropathol. 60: 207, 1983

104. Synder JV, Nemoto EM, Carroll RG, Safar P: Global ischemia in dogs: Intracranial pressure, cerebral blood flow and metabolism. Stroke 6: 21, 1975

105. Hossmann KA, Sakaki S, Kimoto K: Cerebral uptake of glucose and oxygen in the cat brain after prolonged ischemia. Stroke 7: 301, 1976

106. Pulsinelli WA, Levy DE, Duffy TE: Regional cerebral blood flow and glucose metabolism following transient forebrain ischemia. Ann. Neurol. 11: 499, 1982

107. Little J, Kerr F, Sundt T: Microcirculatory obstruction in focal cerebral ischemia: an electron microscope investigation in monkeys. Stroke 7: 25, 1976

108. Miller C, Lampard D, Alexander K, Broen W: Local cerebral blood flow following transient ischemia. Stroke 11: 534, 1980

109. Pulsinelli WA, Brierley J, Plum F: Temporal profile of neuronal damage in a model of transient forebrain ischemia. Ann. Neurol. 11: 491,1982

110. Takagi S, Cocito L, Hossmann KA: Blood recirculation and pharmacological responsiveness of the cerebral vasculature following prolonged ischemia in cat brain. Stroke 8: 707, 1977

111. Mrsulja BB, Mrsulja BJ, Spatz M, Ito U, Walker JT, Klatzo I: Experimental cerebral ischemia in Mongolian gerbils. IV. Behavior of biogenic amines. Acta. Neuropathol. 26: 1, 1976

112. Nemoto EM: Pathogenesis of cerebral ischemia-anoxia. Cri. Care. Med. 6: 203, 1978

113. Suzuki R, Yamaguchi T, Li CL, Klatzo I: The effects of 5 minutes ischemia in Mongolian gerbils: II. changes of spontaneous neuronal activity in cerebral cortex and CA1 sector of hippocampus. Acta. Neuropathol. 60: 217, 1983

114. Ito U, Spatz M, Klatzo I: Experimental cerebral ischemia in Mongolian Gerbils. III. Behavior of the blood-brain barrier. Acta. Neuropathol. 34: 1, 1976

115. Ito U, Ohno K, Inaba Y: Brain edema and regional blood flow during ischemia and after restoration of blood flow. In Gotoh F, Nagai H, Tazaki Y (eds): Cerebral blood flow and metabolism. Ann. Neurol. Scand. Suppl. 72: 264, 1979

116. Ito U, Ohno K, Nakamura R, Suganuma F, Inaba Y: Brain edema during ischemia and restoration of blood flow: measurement of water, sodium, potassium content and plasma protein permeability. Stroke 10: 542, 1979

117. Busto R, Dietrich WD, Globus MYT, Ginsberg MD: Postischemic moderate hypothermia inhibits CA1 hippocampal ischemic neuronal injury. Neurosci. Lett. 101: 299, 1989

118. Minamisawa H, Smith ML, Siesjo BK: The effect of mild hypothermia and hyperthermia on brain damage following 5, 10, and 15 minutes of forebrain ischemia. Ann. Neurol. 28: 26, 1990

119. Mitani A, Kataoka K: Critical levels of extracellular glutamate mediating gerbil hippocampal delayed neuronal death during hypothermia: brain microdialysis study. Neuroscience 42: p661,1991

120. Busto R, Dietrich WD: The importance of brain temperature in cerebral ischemic injury. Stroke 20: 113, 1989

121. Shuaib A, Trulove D, Ijaz MS, Kanthan R, Kalra J: The effect of post-ischemia hypothermia following repetitive cerebral ischemia in gerbils. Neurosci. Lett. 186: 165, 1995

122. Vazquez J: Progressing cerebral infarction in relation to plasma glucose in gerbils. Stroke 21: 1621, 1990

123. Welsh FA, Sims RE, McKee AE: Effect of glucose on recovery of energy metabolism following hypoxia-oligemia in mouse brain: Dose-dependence and carbohydrate specificity. J. Cereb. Blood Flow Metab. 3: 486, 1983

124. Rehncrona S, Rosen I, Siesjo BK: Brain lactic acidosis and ischemic cell damage. J. Cereb. Blood Flow Metab. 1: 297, 1981

125. Gardiner M, Smith ML, Kagstrom E, Shohami E, Siesjo BK: Influence of blood glucose concentration on brain lactate accumulation during sever hypoxia and subsequent recovery of brain energy metabolism. J. Cereb. Blood Flow Metab. 2: 429, 1982

126. Michenfelder JD, Milde JH: Influence of anesthetics on metabolic, functional and pathological responses to regional cerebral ischemia. Stroke 6: 405, 1975

127. Levy DE, Brierley JB: Delayed pentobarbital administration limits ischemic brain damage in gerbils. Annals Neurol. 5: 59, 1979

128. Jarrott DM, Domer FR: A gerbil model of cerebral ischemia suitable for drug evaluation. Stroke 11: 203, 1980

129. Payan HM, Conrad JR: Carotid ligation in gerbils: influence of age, sex and gonads. Stroke 8: 194, 1977

130. Rogers AW: Techniques of autoradiography. Elsevier/north-Holland Biomedical press, Amsterdam, The Netherlands, 1979

131. Lear JL, Ackermann RF, Kameyama M, Kuhl DE: Evaluation of ^{123}I-isopropyliodoamphetamine as a tracer for local blood flow using direct autoradiographic comparison. J. Cereb. Blood Flow Metab. 2: 179, 1982

132. Mastuda H, Tsuji S, Oba H: Direct autoradiographic comparison of ^{99m} Tc-HMPAO with ^{125}I-IMP in experimental brain ischemia. Nuc. Med. Commun. 9: 891, 1988

133. Yoshimine T, Hayakawa T, Yamada K, Takemoto O, Kato A: Regional cerebral ischemia in the gerbil: measurement of regional cerebral blood flow by quantitative autoradiography. J. Cereb. Blood Flow Metab. 6: 348, 1986

134. Ohno K, Ito U, Inaba Y: Regional cerebral blood flow and stroke index after left carotid artery ligation in the conscious gerbil. Brain. Res. 297: 151, 1984

135. Matsumoto M, Hatakeyama T, Fumiharu A, Brengamn JM, Yanagihara T: Prediction of stroke before and after unilateral occlusion of the common carotid artery in gerbils. Stroke. 19: 490, 1987

136. McGraw CP: Experimental cerebral infarction effects of pentobarbital in Mongolian gerbils. Arch. Neurol. 34: 334, 1977

137. Kuroiwa T, Bonnekoh P, Hossmann KA: Therapeutic window of halothane anesthesia for reversal of delayed neuronal injury in gerbils: relationship to postischemic motor hyperactivity. Brain Res. 563: 33, 1991

138. Smith ML, Auer RN, Siesjo BK: The density and distribution of ischemic brain injury in the rat following 2-10 min of forebrain ischemia. Acta. Neuropathol. 64: 319, 1984

139. Kirino T, Tsujita Y, Tamura A: Induced tolerance to ischemia in gerbil hippocampal neurons. J. Cere. Blood Flow Metab. 11: 299, 1991

140. Kuroiwa T, Bonnekoh P, Hossmann KA: Prevention of post-ischemia hyperthermia in prevents ischemic injury of CA1 neurons in gerbils. J. Cere. Blood Flow Metab. 10: 550, 1990

APPENDICES

Appendix 1. Statistic Analysis of the brain uptake in the control and ligation groups in biodistribution study.

Table 1. Brain radioactivity following i.v. administration of ^{125}I-IAZA in the ligation and the control groups (3 animals in each group) at various time intervals.

	2 h	4 h	8 h	24 h
	percentage of injected dose per gram			
control	0.1125±0.0103	0.0363±0.0036	0.0147±0.0005	0.0112±0.0007
ligation	0.1754±0.0784	0.0512±0.0065	0.0298±0.0059	0.0276±0.0021
	brain-to-blood ratios			
control	0.5488±0.0580	0.1826±0.0054	0.1136±0.0042	0.1394±0.0180
ligation	0.5944±0.0674	0.2104±0.0034	0.2703±0.0553	0.2656±0.0255

As it is shown in the above table, the brain uptake in the ligation group is higher than that of the control group. We use two-sample t test to analyze the data and to determine whether there is a significant difference in brain uptake between the two groups. We set a two-sided t test at α=0.05 level of significance.

1) Two-sample t-test on percent of injected dose per gram in the control and ligated gerbils at various time intervals:

2 hr

variable	number	mean	S.D.	df	t	P
control	3	0.1125	0.0103	4	1.379	>0.05
ligation	3	0.1754	0.0784			

4 hr

variable	number	mean	S.D.	df	t	P
control	3	0.0363	0.0036	4	3.473	<0.05
ligation	3	0.0512	0.0065			

8 hr

variable	number	mean	S.D.	df	t	P
control	3	0.0147	0.0005	4	8.291	<0.05
ligation	3	0.0298	0.0059			

24 hr

variable	number	mean	S.D.	df	t	P
control	3	0.0112	0.0007	4	12.833	<0.05
ligation	3	0.0276	0.0021			

2) Two-sample t-test on brain-to-blood ratios at various time intervals:

2hr

variable	number	mean	S.D.	df	t	P
control	3	0.5488	0.0580	4	0.894	>0.05
ligation	3	0.5944	0.0674			

4 hr

variable	number	mean	S.D.	df	t	P
control	3	0.1826	0.0054	4	7.546	<0.05
ligation	3	0.2104	0.0034			

8 hr

variable	number	mean	S.D.	df	t	P
control	3	0.1136	0.0042	4	8.091	<0.05
ligation	3	0.2703	0.0553			

24 hr

variable	number	mean	S.D.	df	t	P
control	3	0.1394	0.0180	4	7.011	<0.05
ligation	3	0.2656	0.0255			

From the above results, we could conclude that :

The brain uptake in the ligation group, in terms of percent of injected dose per gram and brain-to-blood ratios, is significant different from that of the control group at 4hr, 8hr, and 24 hr ($p<0.05$). However, there is no significant difference in brain uptake between the two groups at 2 hr.

Appendix 2. Statistic analysis of the brain section uptake in the control and ligation groups in brain sectioning study.

Table 2. ^{125}I-IAZA uptake in brain sections at 5hr following i.v. administration in the control and ligation groups.

	control (n=1)	ligation A (n=2)	ligation B (n=2)	ligation C (n=3)
stroke index	0	5	10	12
section A	0.0152	0.0200±0.0032[a]	0.0265±0.0024	0.0341±0.0045
	0.0813	0.1018±0.0161[b]	0.1866±0.0131	0.2254±0.0328
section B	0.0178	0.0222±0.0048	0.0348±0.0018	0.0457±0.0033
	0.1035	0.1120±0.0112	0.2457±0.0178	0.3145±0.0204
section C	0.0173	0.0234±0.0064	0.0376±0.0020	0.0454±0.0026
	0.1006	0.1174±0.0159	0.2604±0.0032	0.3182±0.0069
section D	0.0174	0.0224±0.0037	0.0331±0.0027	0.0398±0.0010
	0.1012	0.1140±0.0073	0.2344±0.0109	0.2759±0.0062
section E	0.0178	0.0213±0.0038	0.0267±0.0041	0.0368±0.0019
	0.1035	0.1079±0.0051	0.1899±0.0179	0.2563±0.0121
section F	0.0151	0.0195±0.0052	0.0193±0.0002	0.0208±0.0005
	0.0878	0.1030±0.0040	0.1290±0.0138	0.1306±0.0039
section G	0.0150	0.0185±0.0040	0.0183±0.0039	0.0205±0.0021
	0.0873	0.1022±0.0029	0.1148±0.0181	0.1202±0.0134

a. The values represent the mean±SD for percent of injected dose per gram of brain tissue.

b. The values represent the mean±SD for tissue-to-blood ratio.

From Table 2, we noted that the brain section uptake in the ligation groups was higher than that of the control group. However, with only one control animal, it is mathematically impossible to use the statistic method to compare the control and the ligation groups. Since the ligation groups showed an increased brain section uptake as the stroke index increased, we used one-way ANOVA and Bonferroni multiple comparison procedures to see whether there are significant differences among these groups. The level of significance (α) for overall comparison is 0.05, then the significance level for an individual comparison (ligation group A vs ligation group C) is $\alpha = 0.05/3 = 0.0167$.

1) One-way ANOVA on brain section uptake among ligation groups.

Section A

variable	S_B^2	S_W^2	n-k	k-1	F	P
dose per gram	1.22×10^{-5}	1.41×10^{-5}	4	2	8.65	>0.05
tissue-to-blood ratio	9.25×10^{-3}	6.45×10^{-4}	4	2	14.31	<0.05

Section B

variable	S_B^2	S_W^2	n-k	k-1	F	P
dose per gram	3.33×10^{-4}	1.20×10^{-5}	4	2	27.74	<0.05
tissue-to-blood ratio	2.47×10^{-2}	3.19×10^{-4}	4	2	77.46	<0.05

Section C

variable	S_B^2	S_W^2	n-k	k-1	F	P
dose per gram	2.91×10^{-4}	1.46×10^{-5}	4	2	19.93	<0.05
tissue-to-blood ratio	2.46×10^{-2}	8.96×10^{-5}	4	2	274.55	<0.05

Section D

variable	S_B^2	S_W^2	n-k	k-1	F	P
dose per gram	1.82×10^{-4}	5.47×10^{-6}	4	2	31.71	<0.05
tissue-to-blood ratio	1.61×10^{-2}	6.22×10^{-5}	4	2	258.01	<0.05

Section E

variable	S_B^2	S_W^2	n-k	k-1	F	P
dose per gram	1.55×10^{-4}	9.61×10^{-6}	4	2	16.13	<0.05
tissue-to-blood ratio	1.32×10^{-2}	1.59×10^{-4}	4	2	83.02	<0.05

Section F

variable	S_B^2	S_W^2	n-k	k-1	F	P
dose per gram	1.70×10^{-6}	2.03×10^{-5}	4	2	0.84	>0.05
tissue-to-blood ratio	5.21×10^{-4}	5.92×10^{-5}	4	2	8.81	>0.05

Section G

variable	S_B^2	S_W^2	n-k	k-1	F	P
dose per gram	3.81×10^{-6}	1.01×10^{-5}	4	2	0.38	>0.05
tissue-to-blood ratio	1.97×10^{-4}	1.74×10^{-4}	4	2	1.14	>0.05

2) Analyzing brain section uptake in the ligation A and the ligation C groups by applying Bonferroni multiple comparisons procedures (α=0.0167).

Section A

variable	mean $(X_C - X_A)$	S_W^2	t_{AC}	P
dose per gram	0.0141	1.41×10^{-5}	4.11	>0.02
tissue-to-blood ratio	0.1236	6.45×10^{-4}	5.86	<0.01

Section B

variable	mean $(X_C - X_A)$	S_W^2	t_{AC}	P
dose per gram	0.0235	1.20×10^{-5}	7.44	<0.01
tissue-to-blood ratio	0.2025	3.19×10^{-4}	12.39	<0.01

Section C

variable	mean (X_C–X_A)	S_W^2	t_{AC}	P
dose per gram	0.0222	1.46×10^{-5}	6.31	<0.01
tissue-to-blood ratio	0.2008	8.96×10^{-5}	23.24	<0.01

Section D

variable	mean (X_C–X_A)	S_W^2	t_{AC}	P
dose per gram	0.0174	5.47×10^{-6}	8.13	<0.01
tissue-to-blood ratio	0.1619	6.22×10^{-5}	22.49	<0.01

Section E

variable	mean (X_C–X_A)	S_W^2	t_{AC}	P
dose per gram	0.0155	9.61×10^{-6}	5.89	<0.01
tissue-to-blood ratio	0.1484	1.59×10^{-4}	12.90	<0.01

Section F

variable	mean (X_C–X_A)	S_W^2	t_{AC}	P
dose per gram	0.0013	2.03×10^{-5}	0.32	>0.1
tissue-to-blood ratio	0.0276	5.92×10^{-5}	3.93	>0.1

Section G

variable	mean (X_C–X_A)	S_W^2	t_{AC}	P
dose per gram	0.0020	1.01×10^{-5}	0.69	>0.1
tissue-to-blood ratio	0.0120	1.74×10^{-4}	1.50	>0.1

From the above results, we could conclude that :

There are significant differences in uptake in the forebrain sections (A-E) among the three ligation groups($p<0.05$). The radioactivity in forebrain sections in the ligation group C is also significantly higher ($P<0.01$) than that of the ligation group A. However, there is no significant difference in uptake in the posterior brain sections (F-G) among the ligation groups($P>0.05$).

Appendix 3. Statistic analysis of silver grains in autoradiography study.

Table 3. Mean silver grains per grid (1 mm^2) over autoradiographs in different anatomic sites in both control and ligated gerbils of the first group.

Brain section	control #1	ligation#1	ligation#2	ligation#3	ligation #4
Cortex					
frontparietal	28	64	61	78	79
parietal	25	56	54	69	68
Hippocampus	27	61	62	75	78
Dental gyrus	22	45	44	55	56
Thalamus	26	54	55	70	68
Hypothalamus	24	51	50	64	61
Caudoputamen	26	58	56	72	70
Septal nucleus	25	56	53	68	67

* ligation #1 and #2 were subjected to 5min of bilateral ligation.
* ligation #3 and #4 were subjected to 10min of bilateral ligation.

Table 4. Mean silver grains per grid (1 mm^2) in different anatomic sites in both control and ligated gerbils of the second group.

Brain section	control#2	ligation#5	ligation#6	ligation7	ligation#8
Cortex					
frontal	43	126	105	104	110
frontparietal	46	137	119	112	121
parietal	41	120	99	97	102
Hippocampus	48	145	130	122	132
Dental gyrus	36	103	85	82	87
Thalamus	40	116	95	94	98
Hypothalamus	38	106	91	90	93
Caudoputamen	46	133	111	110	117
Septal nucleus	44	127	106	105	110
Substantia nigra	34	97	81	80	83

From Table 3 and 4 we appear to have a higher grain density in the ligation groups. We analyzed these data by using two-sample t test with the level of significance (α) of 0.05. Since we only have one control animal in each group, we used the data from two brain slices of the control animal to do the calculation.

1) Two-sample t-test on silver grain density in animals of the first group.

a) Control group vs 5 min ligation group

Cortex frontalparietal

variable	number	mean	S.D.	df	t	P
control	2	28	2.12	2	16.27	<0.01
ligation	2	62.5	2.12			

Cortex parietal

variable	number	mean	S.D.	df	t	P
control	2	25	0.71	2	27.03	<0.01
ligation	2	55	1.41			

Hippocampus

variable	number	mean	S.D.	df	t	P
control	2	27	1.41	2	31.08	<0.01
ligation	2	61.5	0.71			

Dental gyrus

variable	number	mean	S.D.	df	t	P
control	2	24	2.12	2	14.24	<0.01
ligation	2	44.5	0.71			

Thalamus

variable	number	mean	S.D.	df	t	P
control	2	26	0.71	2	40.14	<0.01
ligation	2	54.5	0.71			

Hypothalamus

variable	number	mean	S.D.	df	t	P
control	2	24	1.41	2	23.81	<0.01
ligation	2	50.4	0.71			

Caudoputamen

variable	number	mean	S.D.	df	t	P
control	2	26	2.12	2	17.22	<0.01
ligation	2	57	1.41			

Septal nucleus

variable	number	mean	S.D.	df	t	P
control	2	25	1.41	2	16.39	<0.01
ligation	2	54.5	2.12			

b) control group vs 10 min ligation group

Cortex frontalparietal

variable	number	mean	S.D.	df	t	P
control	2	28	2.12	2	31.96	<0.01
ligation	2	78.5	0.71			

Cortex parietal

variable	number	mean	S.D.	df	t	P
control	2	25	0.71	2	61.28	<0.01
ligation	2	68.5	0.71			

Hipocampus

variable	number	mean	S.D.	df	t	P
control	2	27	1.41	2	27.51	<0.01
ligation	2	76.5	2.12			

Dental gyrus

variable	number	mean	S.D.	df	t	P
control	2	24	2.12	2	22.47	<0.01
ligation	2	55.5	0.71			

Thalamus

variable	number	mean	S.D.	df	t	P
control	2	26	0.71	2	38.74	<0.01
ligation	2	69	1.41			

Hypothalamus

variable	number	mean	S.D.	df	t	P
control	2	24	1.41	2	21.39	<0.01
ligation	2	62.5	2.12			

Caudoputamen

variable	number	mean	S.D.	df	t	P
control	2	26	2.12	2	25.01	<0.01
ligation	2	71	1.41			

Septal nucleus

variable	number	mean	S.D.	df	t	P
control	2	25	1.41	2	40.99	<0.01
ligation	2	67.5	0.71			

c) 5 min ligation group vs 10 min ligation group

Cortex frontalparietal

variable	number	mean	S.D.	df	t	P
ligation	2	62.5	2.12	2	10.13	<0.05
ligation	2	78.5	0.71			

Cortex parietal

variable	number	mean	S.D.	df	t	P
ligation	2	55	1.41	2	12.16	<0.05
ligation	2	68.5	0.71			

Hippocampus

variable	number	mean	S.D.	df	t	P
ligation	2	61.5	0.71	2	9.49	<0.05
ligation	2	76.5	2.12			

Dental gyrus

variable	number	mean	S.D.	df	t	P
ligation	2	44.5	2.12	2	15.49	<0.05
ligation	2	55.5	0.71			

Thalamus

variable	number	mean	S.D.	df	t	P
ligation	2	54.5	0.71	2	13.06	<0.05
ligation	2	69	1.41			

Hypothalamus

variable	number	mean	S.D.	df	t	P
ligation	2	50.5	0.71	2	7.59	<0.05
ligation	2	62.5	2.12			

Caudoputamen

variable	number	mean	S.D.	df	t	P
ligation	2	57	1.41	2	18.44	<0.05
ligation	2	71	1.41			

Septal nucleus

variable	number	mean	S.D.	df	t	P
ligation	2	54.5	2.12	2	8.23	<0.05
ligation	2	67.5	0.71			

2) Two-sample t-test on silver grain density in animals of the second group.

control group vs 5 min ligation group

Cortex frontal

variable	number	mean	S.D.	df	t	P
control	2	43	2.83	4	8.45	<0.01
ligation	4	111.25	10.06			

Cortex frontalparieta

variable	number	mean	S.D.	df	t	P
control	2	46	3.61	4	9.45	<0.01
ligation	4	122.25	10.56			

Cortex parietal

variable	number	mean	S.D.	df	t	P
control	2	41	2.83	4	7.95	<0.01
ligation	4	104.5	10.53			

Hippocampus

variable	number	mean	S.D.	df	t	P
control	2	48	3.61	4	11.51	<0.01
ligation	4	132.25	9.54			

Dental gyrus

variable	number	mean	S.D.	df	t	P
control	2	36	2.12	4	7.50	<0.01
ligation	4	89.25	9.39			

Thalamus

variable	number	mean	S.D.	df	t	P
control	2	40	2.83	4	7.76	<0.01
ligation	4	100.75	10.31			

Hypothalamus

variable	number	mean	S.D.	df	t	P
control	2	38	2.12	4	10.07	<0.01
ligation	4	95	7.44			

Caudoputemen

variable	number	mean	S.D.	df	t	P
control	2	46	3.61	4	8.84	<0.01
ligation	4	117.75	10.63			

Septal nucleus

variable	number	mean	S.D.	df	t	P
control	2	44	2.83	4	8.75	<0.01
ligation	4	112	10.23			

Substantia nigra

variable	number	mean	S.D.	df	t	P
control	2	34	2.12	4	8.37	<0.01
ligation	4	85.25	7.93			
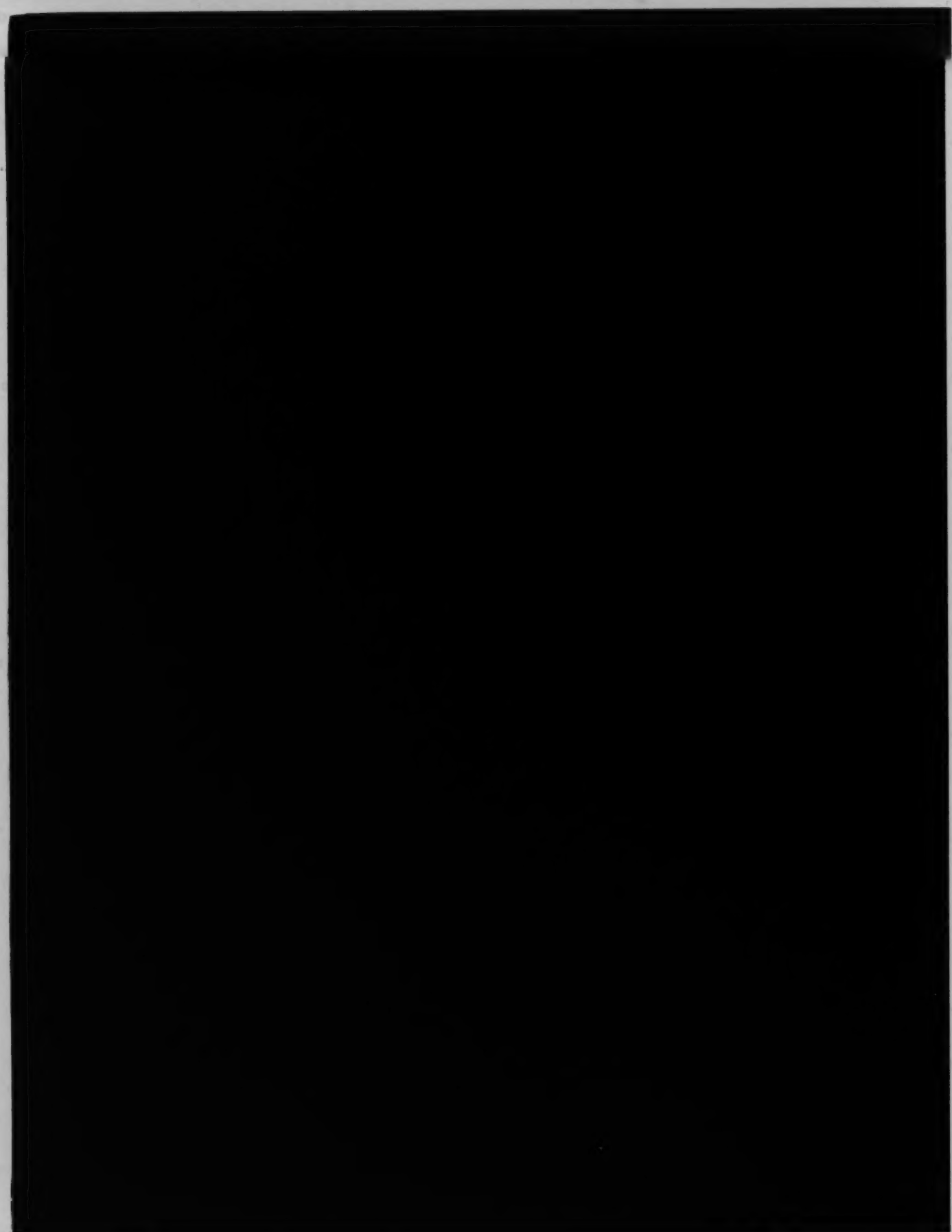
From the above results, we conclude that the silver grain density in ligation group is significant higher than that of the control group ($P<0.01$). On the other hand, there is a significant difference in silver grain density between the 5min ligation group and the 10min ligation groups($P<0.05$).